

STOCHASTIC ANALYSIS OF FLOW AND
SOLUTE TRANSPORT IN A VARIABLE-APERTURE
ROCK FRACTURE

by

David M. Brown

S. B. in Civil Engineering
MIT, 1981

Submitted to the Department of
Civil Engineering
in Partial Fulfillment of the
Requirements of the Degree of

Master of Science

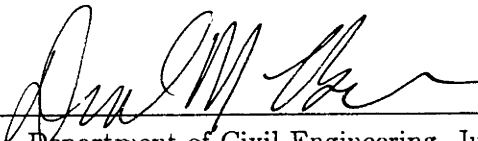
at the

Massachusetts Institute of Technology

June, 1984

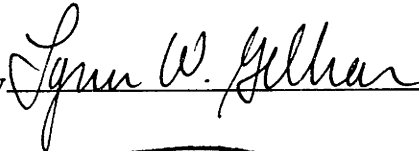
©Massachusetts Institute of Technology 1984

Signature of Author



Department of Civil Engineering, June 30, 1984

Certified by



Thesis Supervisor

Accepted by



Chairman, Graduate Student Committee

ARCHIVES
MASSACHUSETTS INSTITUTE
OF TECHNOLOGY

DEC 27 1984

LIBRARIES

STOCHASTIC ANALYSIS OF FLOW AND
SOLUTE TRANSPORT IN A VARIABLE-APERTURE
ROCK FRACTURE

by

DAVID M. BROWN

Submitted to the Department of Civil Engineering in June 1984
in partial fulfillment of the requirements for the degree Master
of Science in Civil Engineering.

ABSTRACT

Fluid flow and solute transport in a variable-aperture rock fracture are examined using a model of the aperture as a two-dimensional stationary stochastic process and assuming a parabolic velocity profile across the fracture width at each point. The system is cross-sectionally averaged. Effective homogeneous apertures are found which predict the mean velocity and mean flux. The cube of the effective aperture for flux and the square of the effective aperture for velocity are, in general, different tensors. These tensors are functions of the mean, variance and correlation structure of the logaperture process. Effective macrodispersion coefficients are found which are proportional to the mean velocity, the maximum correlation scale, the logaperture variance and functions of the degree and orientation of statistical anisotropy. The effective solute advection velocity has a direction different from the mean velocity and its components are proportional to it, the logaperture variance and functions of the degree and orientation of statistical anisotropy. The component parallel to the mean velocity is always less than or equal to it. This system differs from the two-dimensional porous medium stochastic model in this regard and in the fact that the off-diagonal terms of the dispersion coefficient are nonzero for anisotropic logaperture correlation functions. Existing field data confirms the advection correction effect, but no studies to date have shown evidence of hydraulic or dispersive anisotropy.

Thesis Supervisor
Title

Lynn W. Gelhar
Professor of Civil Engineering

Table of Contents

Table of Contents	2
1. Introduction	4
1.1. Review of single fracture fluid flow	5
1.2. Review of fracture mass transport	9
1.3. Objectives	19
2. Fluid Flow	20
2.1. Head variance	22
2.2. Effective aperture for flux	25
2.3. Effective aperture for velocity	29
3. Solute Transport	31
3.1. Dispersive Model	32
3.2. Decay model	40
4. Summary and Discussion	44
A. Autocovariances and Spectra	50
B. Details of Calculations	52
B.1. Dispersive model with isotropic logaperture process .	52
B.2. Dispersive model with anisotropic logaperture process	57
B.3. Decay model with isotropic logaperture process . . .	60
B.4. Decay model with anisotropic logaperture process . .	62
C. Bibliography	65

FIGURES

Figure 1.1. Flow rate vs. stress	6
Figure 1.2. Test of cubic law	8
Figure 1.3. Dyestreaks in a fracture	9
Figure 1.4. Geometry for matrix diffusion model	12
Figure 1.5. Matrix diffusion breakthroughs	17
Figure 1.6. Breakthrough curve in fractured till	18
Figure 2.1. Correlation structure for flow problem	23
Figure 2.2. Autocovariance functions	25
Figure 3.1. Correlation structure for mass transport problem .	33
Figure 3.2. Definition of \tilde{u}_i	42

TABLES

Table 1.1. Matrix diffusion papers	16
--	----

Chapter 1.

Introduction

Many problems in groundwater hydrology involve fractured rock aquifers. For example, contamination sites often involve fractured regimes, geothermal energy can be extracted from hot dry fractured rocks underground, and crystalline rock masses are being considered for high level radioactive waste isolation. In spite of this and fifteen years of research, little is known about the proper way to model fractured rock systems.

Hydrologists usually attempt to apply some sort of continuum model to such a system, since that greatly simplifies their analyses. In some cases, though, such as waste isolation, it is necessary to account for the effect of individual discontinuities on the hydrologic regime. Sites for waste isolation are usually evaluated on their tightness, that is, their lack of fractures. No site is completely free of fractures, however, and thus the hydrology of those fractures that exist will be dominated by discrete pathways and a continuum model will probably not be appropriate. Moreover, research into the conditions under which a continuum model will work often depends on an accurate understanding of the processes controlling discrete systems. Analytical and numerical field scale solute transport models also depend on an understanding of the physics of transport in individual fractures.

1.1. Review of single fracture fluid flow

Most researchers have modeled flow in a single fracture as flow between a pair of parallel plates. This approach was first developed extensively by D. T. Snow in a series of papers in the late 1960s (*Snow* (1966, 1968a, 1968b, 1968c, 1969, 1970), *Bianchi and Snow*, (1968)). In this model, which presumes full-developed laminar flow with a parabolic velocity profile, the average fluid velocity, u , over the fracture cross-section is given by

$$u = \frac{b^2 g J}{12\nu}, \quad (1.1)$$

where b is the fracture's aperture, g is the gravitational acceleration, ν is the kinematic viscosity and J is the magnitude of the hydraulic gradient.

Thus, for a unit width perpendicular to both the fluid velocity and the plane of the fracture, the total flow, Q , is given by

$$Q = \frac{b^3 g J}{12\nu}, \quad (1.2)$$

which is the well-known "cubic law" relating flow to aperture. The logical definition of definition of fracture hydraulic conductivity, K_f , is then

$$K_f = \frac{b^2 g}{12\nu}. \quad (1.3)$$

This is the conductivity of only the volume of space occupied by fractures.

In the case that the fracture walls are considered to have a finite roughness, *Castillo et. al.* (1972), suggest that known relationships between friction factor and Reynolds number for flow in circular pipes be used, with the definition of the Reynolds number as

$$\mathbf{R} = \frac{4bu}{\nu}. \quad (1.4)$$

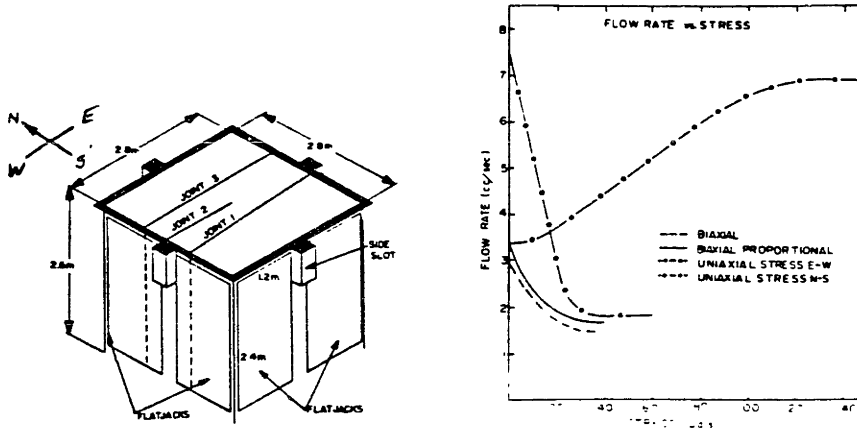


Figure 1.1: Variation of flow rate in natural fracture with different stresses. *Pratt et. al. (1977)*.

Alternatively, *Rocha and Franciss (1977)* report *Louis' (1969)* empirical result

$$K_f = \frac{b^2 g}{12\nu} \left(\frac{1}{1 + 8.8r^{1.5}} \right) \quad (1.5)$$

where r is the relative roughness of the fracture walls.

Of course, we know that fracture walls are not perfectly parallel, since a fracture will conduct flow while the walls are subjected to normal stress. There must, then, be places of contact where this stress is endured, while other areas are not in contact, permitting flow.

Pratt et. al. (1977) studied the stress dependence of flow in three granite fractures in the field. They found that even after the fracture was closed (in that its modulus of elasticity was the same as for intact rock) a significant amount of flow was still occurring. At low stress, the fracture flow varied enormously, probably due to the cubic law. However, for stresses above 30 bars, there was little or no decrease in flow for large increases in stress (Figure 1.1). Laboratory tests by *Nelson and Handin (1977)*, *Kranz et. al. (1979)*, *Gangi (1978)* and *Witherspoon et. al. (1980)* have all confirmed this behavior.

Witherspoon et. al. (1979) noted a scale effect on the asymptotic value of K_f for high stress. It appears that the larger the sample, the higher the asymptotic value. They hypothesize that this is due to the possibility that the smaller samples do not contain a statistically significant sample of the asperity height distribution. A larger specimen is more likely to sample asperities from the tail of the distribution, which would tend to keep the fracture propped wider for the same stress, thus producing a greater fracture conductivity.

When the aperture in a fracture varies from point to point, it becomes unclear as to which value to use in the cubic law to calculate flow. One alternative is to define the “effective aperture” as

$$\hat{b} = \left(\frac{12Q\nu}{gJ} \right)^{1/3}, \quad (1.6)$$

but this is really a tautology. *Witherspoon et. al.* (1980) sought to find another way to measure the aperture in the lab, and in doing so found an independent check of the cubic law.

Their method was to subject a fracture specimen to uniaxial stress while measuring the strain across both the fracture and portions of the intact rock. By subtracting the deformation of the intact rock from the total deformation, it was possible to deduce the deformation in the fracture. Figure 1.2 shows the relationship between this deformation and the fracture’s aperture. The total aperture, b , is equal to the sum of the apparent aperture, b_d , and the residual aperture, b_r . When the fracture is closed, $b_d = 0$, but there is still flow, corresponding to the residual aperture. The cubic law was then rewritten as

$$\frac{Q}{J} = \frac{g}{12\nu}(b_d + b_r)^n, \quad (1.7)$$

where n and b_r are the unknowns, to be estimated from the stress-flow data. The result was that in every case, the exponent n came very close to 3, thus validating the cubic law for fractures whose walls are in contact at places.

Another approach is to attempt to specify the aperture at every point in the fracture and then solve for the flow analytically. Simplifying assumptions are in order. For example, *Neuzil and Tracy* (1981)

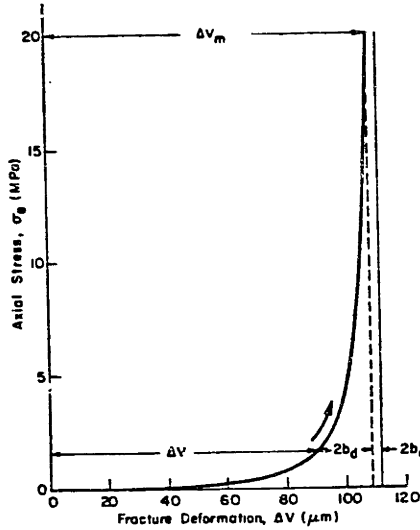


Figure 1.2: Relationship between apparent aperture, residual aperture, total deformation and stress in a variable-aperture fracture. Total deformation, ΔV_m , is equal to total aperture minus residual aperture. *Witherspoon, et. al. (1980)*

have assumed that the aperture may be considered to vary orthogonally to the flow, but is constant in the direction parallel to the flow. Then, the effective aperture turns out to be the cube root of the mean of the aperture distribution cubed:

$$\hat{b} = (\overline{b^3})^{1/3}, \quad (1.8)$$

where the overbar represents the expected value. This is what we expect in analogy with a set of resistors in parallel. *Tsang and Witherspoon (1981)* also derived (1.8) for variation orthogonal to the flow. In order to analyze the effect of variation along the flow path, it is necessary to integrate the total drop in head longitudinally, and then relate the constant flux, Q , to the mean hydraulic gradient, concluding that

$$\hat{b} = (\overline{b^{-3}})^{-1/3}. \quad (1.9)$$

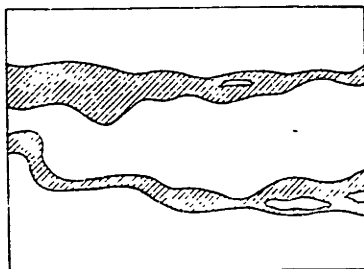


Figure 1.3: Dyestreaks in a fracture. *Neuzil and Tracy (1981)*, from *Louis (1969)*.

However, these quasi-two-dimensional analyses are only partially correct since they do not allow for flow or gradient direction to vary, whereas it is well-known that in a two-dimensional conductivity field, flow is diverted around areas of low conductivity. In fact, Figure 1.3 (Figure 1 in *Neuzil and Tracy (1981)*, from *Louis (1969)*), shows such a two-dimensional flow field. They claim that it supports their hypothesis that flow along streamlines occurs in regions of essentially constant aperture. It seems more plausible, though, that this evidence supports a fully two-dimensional model, since the evidently random variation in streamtube width and direction is inherently due to a variable aperture. The analysis of flow in a fracture with a two-dimensionally varying aperture is the subject of chapter 2 of this paper.

1.2. Review of fracture mass transport

In a parallel-plate fracture with impermeable non-porous walls, we expect that the assumed parabolic velocity profile will tend to disperse any solute longitudinally. In addition, we expect that, along the lines of *Taylor's (1953)* analysis, after an appropriate start-up time, molecular diffusion will quickly reduce any transverse concentration

gradient across the aperture and cause the dispersion coefficient to reach a constant value. In a capillary tube, this value is

$$E = \frac{d^2 u^2}{190 D_m}, \quad (1.10)$$

where d is the diameter of the tube, D_m is the coefficient of molecular diffusion and u is the radially-averaged velocity in the tube. *Elder* (1965) provided a way to calculate this for a pair of parallel plates. The result is

$$E = \frac{b^2 u^2}{210 D_m}, \quad (1.11)$$

where now u is the cross-sectionally averaged fluid velocity in the fracture. That this value is slightly lower is reasonable, since there is less of a velocity variation across the cross-section. *Karadi et al.* (1972) presented a method of calculating the average concentration in a fracture at a point downstream from an arbitrarily time-varying input boundary condition, assuming a constant longitudinal dispersivity.

Very little field or lab data exists on single-fracture dispersivities. *Novakowski et al.* (1984) used a two-well tracer test and found a dispersivity of 1.55 m. for an interwell distance of 10.6 m. *Gustaffson and Klockars* (1981) performed a two-well tracer test in fractured rock at Studsvik, in Sweden, finding dispersivities on the order of 1 m. for an interwell distance of 30 m. *Carlsson et al.* (1979) also performed a two-well tracer test, but did not report a dispersivity. Laboratory tests by *Grisak et al.* (1980) and *Neretnieks* were inconclusive regarding dispersivities, but nevertheless found values of 0.15 m. and 0.025 m., respectively. All of these results are discussed in chapter 4.

Much research has emphasized the concept of diffusive transport in the porous but relatively impervious rock matrix bounding the fracture flow, i.e., the so-called "matrix diffusion" model. Analytical and laboratory studies include *Grisak et al.* (1980), *Grisak and Pickens* (1980, 1981), *Uffink* (1983), *Tang et al.* (1981), *Sudicky and Frind* (1982, 1984), *Rasmuson and Neretnieks* (1981), *Neretnieks* (1980, 1983), *Neretnieks et al.* (1982), *Erickson* (1981), *Barker* (1982) and *Barker and Foster* (1981). Numerical studies include *Kanki et al.*

(1980), *Noorishad and Mehran* (1982), *Rasumson et. al.* (1982) and *Huyakorn et. al.* (1983a, 1983b). Field experiments which clearly demonstrate the matrix diffusion effect are nonexistent to date. Each model has different features but the essence is the same. Mathematically the model consists of two coupled one-dimensional second-order differential equations. One describes transport longitudinally in the fracture and the other describes diffusion transversely, but without advection, into the porous rock matrix bounding the fracture.

Referring to the geometry of Figure 1.4, the mass balance equations, with all features added, are:

$$\frac{\partial c_f}{\partial t} + u' \frac{\partial c_f}{\partial x} = D'_L \frac{\partial^2 c_f}{\partial x^2} - K c_f - \frac{2D'_m}{b} \left(\frac{\partial c_m}{\partial z} \right)_{z=b/2} \quad (1.12)$$

$$\frac{\partial c_m}{\partial t} = D'_m \frac{\partial^2 c_m}{\partial z^2} - K c_m \quad (1.13)$$

$$u' = u/R_{df} \quad (1.14)$$

$$D'_L = D_L/R_{df} \quad (1.15)$$

$$D'_m = D_m/R_{dm} \quad (1.16)$$

where $c_f = c_f(x, t)$ is the contaminant concentration in the fracture, $c_m = c_m(x, z, t)$ is the concentration in the rock matrix, D_L is the longitudinal dispersion coefficient in the fracture, R_{df} is the retardation factor for solution on the fracture walls, R_{dm} is the matrix retardation factor and K is the species' decay constant. Decay chains can also be accounted for (e. g., *Kanki et. al.*(1980), *Sudicky and Frind* (1984)).

The initial and boundary conditions are:

$$c_f(x, 0) = c_m(x, z, 0) = 0 \quad (1.17)$$

$$c_f(x, t) = c_m(x, b/2, t) \quad (1.18)$$

$$c_f(\infty, t) = c_m(\infty, z, t) = 0 \quad (1.19)$$

$$c_f(0, t) = g(t) \quad (1.20)$$

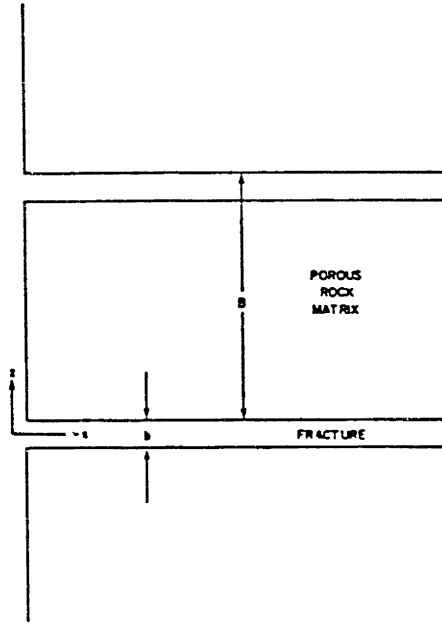


Figure 1.4: Idealized geometry for matrix diffusion model

with one of the following:

$$c_m(x, \infty, t) = 0 \quad (1.21)$$

or

$$\frac{\partial}{\partial z} c_m(x, B/2, t) = 0, \quad (1.22)$$

where $g(t)$ is an arbitrary release scenario and B is the spacing between fractures in a set. Condition (1.22) is used in cases when the lateral boundary has an effect, i.e., when

$$\frac{B}{2} \leq \sqrt{D_m \tau}, \quad (1.23)$$

where τ is the travel time for a pulse of contaminant to pass through the fracture. Otherwise, condition (1.21) may be used. Table 1.1

compares the features and solution techniques for the several matrix diffusion models reported.

It is interesting to compare the matrix diffusion models to the traditional advection-dispersion model. In general, the matrix diffusion model predicts much later breakthroughs and much lower concentrations (Figure 1.5), due to a retarding effect whereby the front of a pulse in the fracture loses mass to the matrix while the tail of a pulse receives mass from the matrix. Whether this can be represented by a single retardation factor is not clear. *Barker and Foster* (1981) showed that when $D'_m \rightarrow \infty$, the concentration is constant in the z -direction, the mass being instantaneously shared between the fracture and matrix pore space. The peak of a pulse would travel with a velocity given by

$$u' = \frac{u}{R_{df}} \left(\frac{b}{b + B\varphi} \right), \quad (1.24)$$

where φ is the porosity of the matrix. Then the fracture may be considered to have an effective retardation factor

$$\widehat{R}_{df} = R_{df} \left(\frac{b + B\varphi}{b} \right). \quad (1.25)$$

However, when D'_m is low enough to affect the problem, as in most real situations, an originally Gaussian profile in the fracture becomes increasingly skewed towards the upstream side. *Neretnieks* (1983) discussed this trend for the case when $D_L = 0$. *Neretnieks* calculated the first and second moments of this breakthrough, and concluded that since the second moment is infinite no advection-dispersion model can fit the curve. This is incorrect, though, since it is the spatial moments which should be calculated when using the method of moments. This indicates a need for more careful analysis. It seems possible that some type of time-varying retardation factor and dispersion coefficients could yet represent the physics of this situation. In addition, for some limiting cases, such as small B or large D'_m or travel time τ , Taylor's analysis would again become valid since the storage space in the matrix would have little effect.

Author(s)	solution technique	a	b	c	d	comments
<i>Barker, 1982</i>	analytical	T	yes	1.21	yes	-
<i>Barker and Foster, 1981</i>	analytical, numerical	T	yes	1.21	no	chromatography analogy, infiltration
<i>Erickson, 1981</i>	analytical	T	no	-	no	spherical diffusion
<i>Grisak and Pickens, 1980</i>	analytical, numerical	T	yes	1.21	no	-
<i>Grisak and Pickens, 1981</i>	analytical	T	no	1.22	no	-
<i>Grisak et. al., 1980</i>	laboratory	T	yes	1.21	no	-
<i>Huyakorn et. al., (1983a)</i>	numerical	T	yes	1.21	yes	spherical or rectilinear diffusion
<i>Huyakorn et. al., (1983b)</i>	numerical	T	yes	1.21	yes	decay chains, spherical or rectilinear diffusion

^asteady (S) or transient (T)?

^blongitudinal dispersivity in fracture?

^cmatrix boundary condition

^ddecay?

Author(s)	solution technique	<i>a</i>	<i>b</i>	<i>c</i>	<i>d</i>	comments
<i>Kanki et. al., 1980</i>	analytical	T	no	1.22	yes	decay chains
<i>Neretnieks, 1980</i>	analytical	T	no	1.22	yes	decay chains
<i>Neretnieks, 1983</i>	analytical	T	-	1.22	no	advection-dispersion comparison
<i>Neretnieks et. al., 1982</i>	laboratory	T	-	1.21	yes	channeling
<i>Noorishad and Mehran, 1982</i>	numerical	T	yes	1.21	no	-
<i>Rasmuson and Neretnieks, 1981</i>	analytical	T	yes	-	yes	spherical diffusion
<i>Rasmuson et. al., 1982</i>	numerical	T	yes	-	yes	spherical diffusion
<i>Sudicky and Frind, 1982</i>	analytical	S, T	yes	1.22	no	-

^asteady (S) or transient (T)?

^blongitudinal dispersivity in fracture?

^cmatrix boundary condition

^ddecay?

Author(s)	solution technique	<i>a</i>	<i>b</i>	<i>c</i>	<i>d</i>	comments
<i>Sudicky and Frind, 1984</i>	analytical	T	no	1.22	yes	two-member decay chain
<i>Tang et. al., 1981</i>	analytical	S, T	yes	1.21	no	-
<i>Uffink, 1983</i>	analytical	T	no	1.22, 1.21	no	heat flow

^asteady (S) or transient (T)?

^blongitudinal dispersivity in fracture?

^cmatrix boundary condition

^ddecay?

Table 1.1: Matrix diffusion papers

Grisak et. al. (1980) ran a tracer experiment in the lab using both reactive and non-reactive solutes and a step input. Their breakthrough curve is shown in Figure 1.6. They concluded that simple advection-dispersion solutions could not fit the breakthrough curves with realistic parameters, whereas matrix diffusion solutions could, albeit roughly. They used condition (1.22) with $B = 3$ cm. and a step input of concentration c_0 . However, the maximum distance of diffusion into the matrix was only 0.36 cm., indicating that the boundary was not reached. This is further borne out by the fact that the breakthrough concentrations reached only about 80% of c_0 , indicating that some mass has not yet left the matrix. They were unaware then of the results of chapter 3 of this report, which predicts a retardation due to aperture variability. In chapter 4, it is shown that the parameters used to fit the advection-dispersion model may be more realistic than seems at first glance.

In fitting their matrix diffusion models, *Grisak et. al.* (1980) used a longitudinal dispersivity of 76 cm., the length of their column. In fact, they had little idea what value to use, their choice being

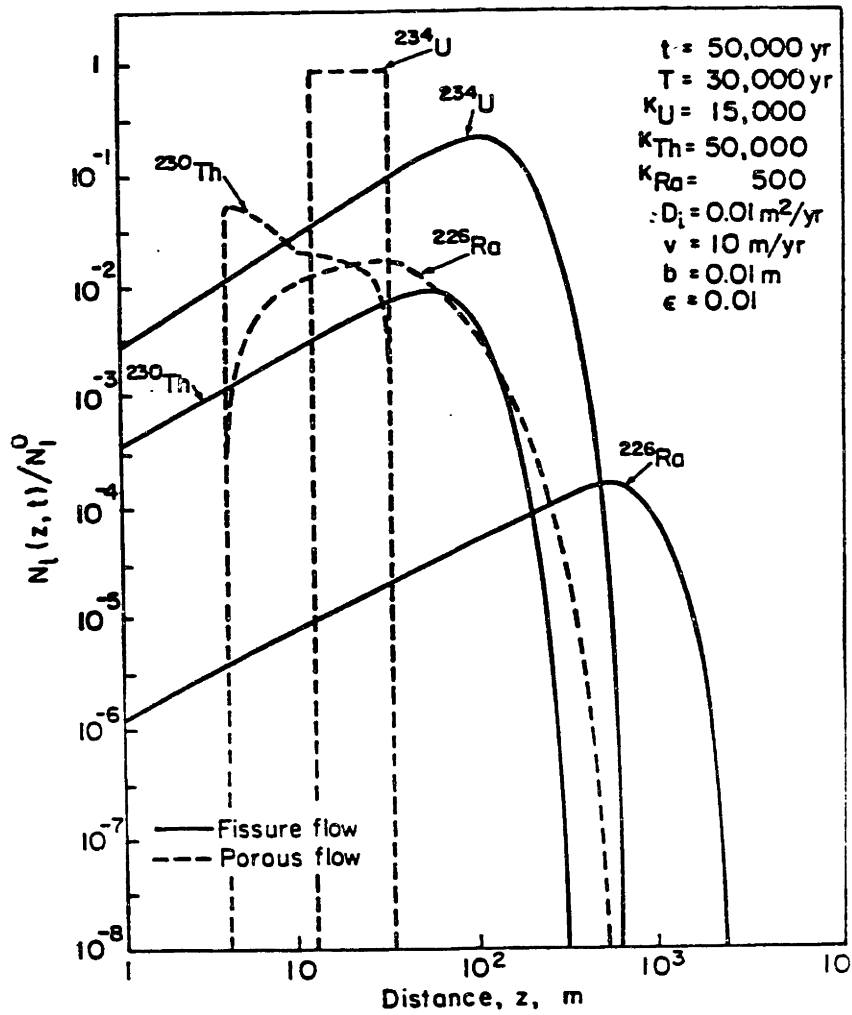


Figure 1.5: Radionuclide decay chain breakthroughs for advection-dispersion (dashed line) and matrix diffusion (solid line) models. Kanki et. al. (1980).

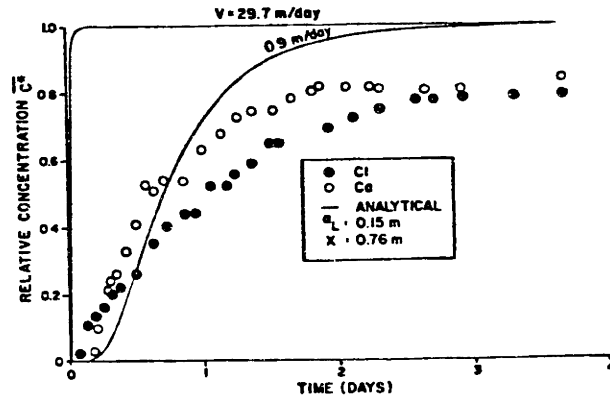


Figure 1.6: Breakthrough curve in fractured till and attempts to fit advection-dispersion model to it. *Grisak et. al.* (1980).

based mostly on heuristical reasoning (*Grisak, 1984*). This points out the need for good estimates of dispersivities to be used as input for these matrix diffusion models. Chapter 3 of this paper uses the results of the two-dimensional stochastic flow analysis to calculate such dispersivities.

1.3. Objectives

The objective of this report is to formally evaluate the effect of aperture variation on fracture flow and mass transport. This will be done by modeling the logaperture as a two-dimensional stationary stochastic process.

This method has met with some success in two-dimensional porous medium models of aquifer heterogeneity (*Mizell et. al. (1982), Gelhar and Axness (1983)*). *Mizell et. al. (1982)* looked at a two-dimensional flow in a confined aquifer with variable transmissivity and *Gelhar and Axness (1983)* studied flow and mass transport for a multi-dimensional porous medium with variable hydraulic conductivity. In these papers, heterogeneous systems were modeled by effective homogeneous systems in terms of fluid flux and mass transport. The methods predict, for example, an equivalent hydraulic conductivity for calculating specific discharge and macrodispersion coefficients for large-scale natural systems. As will be seen, however, application of the method to a variable-aperture fracture yields a couple of new twists.

Chapter 2.

Fluid Flow

In this chapter, fluid flow in a variable-aperture fracture is analyzed stochastically, with the aim of finding effective homogeneous apertures for deriving fluid velocities or fluxes. These are useful for interpreting field data, as will be discussed in chapter 4.

The basic assumption of the model in this paper is that the aperture, $b(x, y)$, is a two-dimensional stochastic process. The process is assumed to be second-order stationary in that its mean and variance do not vary over the domain. For convenience, the underlying process is assumed to lognormal, so that the natural logarithm of the aperture function is a Gaussian process, which has only two nonzero moments. The correlation structure of the process is in general anisotropic, and can be represented by any of the four functions described in Appendix A. Usually, the exponential, which is the simplest, is used, but this is not always possible.

The other important assumption is that the cubic law holds at each point. This depends on whether or not the velocity distribution at each point is a parabola. *Langlois* (1964) developed an analysis for one-dimensional flow through a channel of varying width. By solving the Navier-Stokes equations for slow viscous flow, he was able to write the vertical distribution of horizontal velocity as a power series in the assumed small parameter

$$\varepsilon \equiv \left| \frac{db}{dx} \right|. \quad (2.1)$$

This series is

$$u = \left(\frac{3Q}{2b}\right) \left(1 - \frac{4z^2}{b^2}\right) \left[1 + \varepsilon^2 \left(\frac{2}{5} - \frac{8z^2}{b^2}\right) + \mathcal{O}(\varepsilon^3)\right]. \quad (2.2)$$

The absence of the linear (ε^1) term means that the parabolic approximation is good for $\varepsilon^2 \ll 1$. The logical extension to two dimensions is

$$|\nabla b|^2 \ll 1 \quad (2.3)$$

and this will be assumed of the aperture process. Then, the cross-sectionally averaged velocity at any point is proportional to the square of the aperture at that point and is in the direction of the hydraulic gradient:

$$\mathbf{u} = -\frac{b^2 g}{12\nu} \nabla \phi, \quad (2.4)$$

where the del operator is in two dimensions and ϕ is the piezometric head. The fluid flux vector \mathbf{Q} is given by:

$$\mathbf{Q} = -\frac{b^3 g}{12\nu} \nabla \phi. \quad (2.5)$$

This is the single-fracture equivalent of the Darcy equation. The adoption of the cubic law here is rather like the assumption of Representative Elementary Volumes for porous media. The REV concept is used in porous media so that a continuum model may be employed, where the conductivity or porosity of the medium is a function only of the point of interest, and not of the state of its neighborhood. The motivation here is identical, where we desire to neglect the effect of aperture convergence and divergence on the point value of the aperture conductivity.

The equation of continuity for steady flow is

$$\nabla \cdot \mathbf{Q} = \nabla \cdot (b\mathbf{u}) = 0, \quad (2.6)$$

which, using (2.4), can be rewritten

$$\nabla^2 \phi + 3\nabla \phi \cdot \nabla (\ln b) = 0. \quad (2.7)$$

This is in the same form as equation (2) of *Mizell et. al.* (1982), who analyzed a two-dimensional vertically-averaged heterogeneous aquifer, with $\ln b$ taking the place of $\ln T$. The only difference is the factor of 3 appearing in (2.7), which is due to the cubic law. This factor, arising due to the non-linear (cubic) ‘‘Darcy’’ equation accounts for almost all of the differences between this model and the porous medium results.

2.1. Head variance

To illustrate these differences, we take a detour to calculate the variance in head in the fracture due to the variance in aperture. We write the logaperture and head as the sums of their means and their zero-mean perturbations:

$$\ln b = B + \beta(x_1, x_2), \quad (2.8)$$

$$\phi = \bar{H}(x_1) + h(x_1, x_2), \quad (2.9)$$

where B , the mean of $\ln b$, is constant, and $H(x_1)$, the mean of ϕ , is linear. Define J , the mean gradient, as

$$J \equiv -\frac{\partial H}{\partial x_1} \neq 0. \quad (2.10)$$

Note that the x_1 -coordinate has been aligned with the direction of J , as in Figure 2.1. Substituting these into (2.7), we get

$$\nabla^2 h - 3J \frac{\partial \beta}{\partial x_1} + 3\nabla h \cdot \nabla \beta = 0. \quad (2.11)$$

Taking (2.11) and subtracting its mean

$$3\overline{\nabla h \cdot \nabla \beta} = 0, \quad (2.12)$$

(where the overbar signifies the expected value) from it, we obtain the perturbation equation

$$\nabla^2 h - 3J \frac{\partial \beta}{\partial x_1} + 3(\nabla h \cdot \nabla \beta - \overline{\nabla h \cdot \nabla \beta}) = 0. \quad (2.13)$$

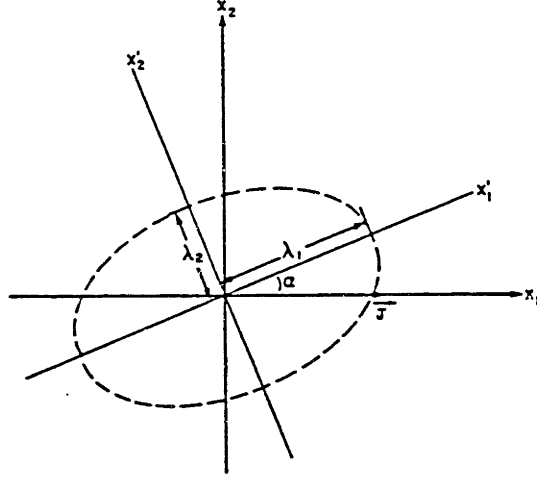


Figure 2.1: Orientation of correlation structure with respect to mean hydraulic gradient.

By assuming that the perturbations h and β are small, the term in parentheses may be neglected. The first-order approximation of the perturbation equation is then

$$\nabla^2 h - 3J \frac{\partial \beta}{\partial x_1} = 0. \quad (2.14)$$

The assumption of stationarity (statistical homogeneity) allows us to write h and β in terms of their Fourier-Stieltjes representations (*Lumley and Panofsky, 1964*):

$$h = \int_{\mathbf{k}} e^{i\mathbf{k}\cdot\mathbf{x}} dZ_h(\mathbf{k}) \quad (2.15)$$

$$\beta = \int_{\mathbf{k}} e^{i\mathbf{k}\cdot\mathbf{x}} dZ_\beta(\mathbf{k}). \quad (2.16)$$

The vector \mathbf{k} is the two-dimensional wave number, and $dZ_h(\mathbf{k})$ and $dZ_\beta(\mathbf{k})$ are the complex Fourier amplitudes of h and β , respectively.

The spectrum of a stochastic process, a , can be determined from its complex Fourier amplitude by

$$S_{aa}(\mathbf{k})d\mathbf{k} = \overline{dZ_a(\mathbf{k})}dZ_a^*(\mathbf{k}), \quad (2.17)$$

where the asterisk denotes the complex conjugate. Similarly, the cross-spectrum of two processes, a and b , is

$$S_{ab}(\mathbf{k})d\mathbf{k} = \overline{dZ_a(\mathbf{k})}dZ_b^*(\mathbf{k}). \quad (2.18)$$

Substituting (2.15) and (2.16) into (2.14) we arrive at

$$dZ_h(\mathbf{k}) = -\frac{3iJk_1}{k^2}dZ_\beta(\mathbf{k}), \quad (2.19)$$

and thus,

$$S_{hh}(\mathbf{k}) = \frac{9J^2k_1^2}{k^4}S_{\beta\beta}(\mathbf{k}), \quad (2.20)$$

gives the transfer function between the spectra of h and β . Here, $k^2 = k_1^2 + k_2^2$.

Now, the variance of a process is equal to the integral of its spectrum over the entire wave number domain. Thus,

$$\sigma_h^2 = \int_{\mathbf{k}} \frac{9J^2k_1^2}{k^4}S_{\beta\beta}(\mathbf{k})d\mathbf{k} \quad (2.21)$$

Appendix A describes four autocovariances and their spectra. These are the exponential, Whittle, Whittle A and Whittle B spectra. All four covariances have approximately the same shape (Figure 2.2), except that the Whittle A and B covariances go negative and approach zero from below. *Mizell et. al.* (1982), found that using either of the first two for f , the perturbation of the log-transmissivity, including the conceptually simple exponential, led to infinite head variance. Using the Whittle A or B, though, they obtained a finite variance.

As might be expected, the same results occur here. The head variance resulting from the Whittle A spectrum for β is

$$\sigma_h^2 = \frac{9J^2\lambda_1\lambda_2}{2\eta^2}\sigma_\beta^2, \quad \eta = \pi/4, \quad (2.22)$$

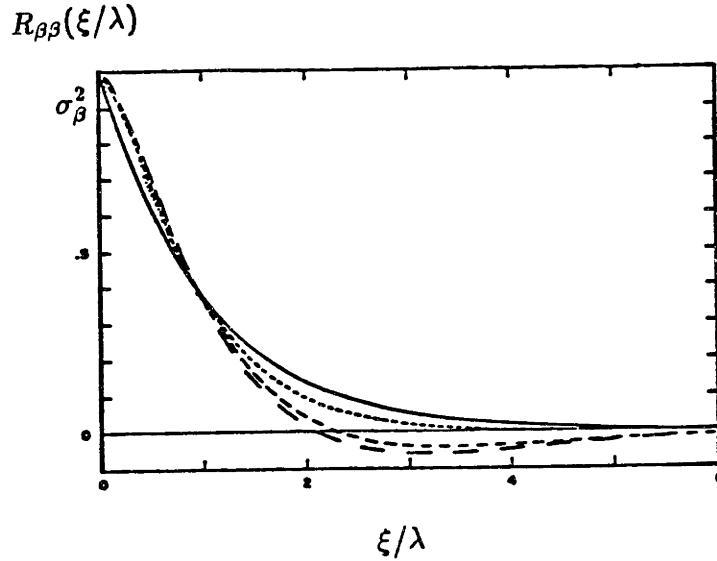


Figure 2.2: Autocovariance functions for exponential (solid line), Whittle (short-dashed line), Whittle A (medium-dashed line) and Whittle B (long-dashed line) with respect to the dimensionless lag, ξ/λ , in a given direction.

and the Whittle B spectrum produces

$$\sigma_h^2 = \frac{9J^2\lambda_1\lambda_2}{4\eta^2}\sigma_\beta^2, \quad \eta = 3\pi/16. \quad (2.23)$$

For the isotropic case ($\lambda_1 = \lambda_2 = \lambda$) these results are exactly what *Mizell et. al.* (1982) found, except for the factor of 9. That the head variance is larger here is not surprising, since the system is steady ($\nabla \cdot \mathbf{Q} = 0$) and fluid flux depends on the aperture cubed, causing ϕ to vary widely with b .

2.2. Effective aperture for flux

The effective aperture for flux is that equivalent homogeneous aperture which predicts the same fluid flux as the mean flux in our heterogeneous aperture system.

Now, the mean flux in the x_1 direction is

$$\overline{Q_1} = \overline{bu_1} = -\frac{g}{12\nu} \overline{b^3 \frac{\partial \phi}{\partial x_1}}. \quad (2.24)$$

Writing $\ln b$ and ϕ in terms of their means and perturbations, and for

$$b_\ell \equiv e^B, \quad (2.25)$$

we have

$$\overline{Q_1} = -\frac{b_\ell^3 g}{12\nu} \overline{e^{3\beta} \frac{\partial(H+h)}{\partial x_1}}. \quad (2.26)$$

Expanding the exponential into its Taylor series, and noting that

$$\overline{\beta^2} = \sigma_\beta^2 \quad (2.27)$$

brings us eventually to the second-order approximation

$$\overline{Q_1} = \frac{b_\ell^3 g}{12\nu} \left[\left(1 + \frac{9}{2}\sigma_\beta^2\right) J - 3\beta \overline{\frac{\partial h}{\partial x_1}} \right]. \quad (2.28)$$

The last term is a cross-covariance, which is evaluated by integrating its cross-spectrum. For $y_1 = \partial h / \partial x_1$,

$$dZ_{y_1}(\mathbf{k}) = ik_1 dZ_h(\mathbf{k}) = \frac{3Jk_1^2}{k^2} dZ_\beta(\mathbf{k}), \quad (2.29)$$

and

$$S_{\beta y_1}(\mathbf{k}) = \frac{3Jk_1^2}{k^2} S_{\beta\beta}(\mathbf{k}), \quad (2.30)$$

and thus,

$$\overline{\beta \frac{\partial h}{\partial x_1}} = \int_{\mathbf{k}} S_{\beta y_1}(\mathbf{k}) d\mathbf{k} = \int_{\mathbf{k}} \frac{3Jk_1^2}{k^2} S_{\beta\beta}(\mathbf{k}) d\mathbf{k}. \quad (2.31)$$

In this case, all four spectra produce the same results:

$$\overline{\beta \frac{\partial h}{\partial x_1}} = 3J\sigma_\beta^2 \left(\frac{\rho \sin^2 \alpha + \cos^2 \alpha}{\rho + 1} \right), \quad (2.32)$$

where $\rho = \lambda_1/\lambda_2$, and α is the angle between the x_1 and x'_1 directions, so that

$$\overline{Q_1} = \frac{b_l^3 g J}{12\nu} \left\{ 1 + \sigma_\beta^2 \left[\frac{9}{2} - 9 \left(\frac{\rho \sin^2 \alpha + \cos^2 \alpha}{\rho + 1} \right) \right] \right\}. \quad (2.33)$$

For the special case of an isotropic logaperture autocovariance, $\rho = 1$, and

$$\overline{Q_1} = \frac{b_l^3 g J}{12\nu}, \quad (2.34)$$

so that the effective aperture is the geometric mean of the aperture process. The same result is had, of course, when $\sigma_\beta^2 = 0$, where now the geometric mean is, trivially, the parallel-plate aperture. When $\alpha = 0$ and $\rho \rightarrow \infty$, we have the same model as *Neuzil and Tracy* (1981), and

$$\overline{Q_1} = \frac{b_l^3 g J}{12\nu} \left(1 + \frac{9}{2} \sigma_\beta^2 \right) \cong \frac{b_l^3 g J}{12\nu} \exp \left(\frac{9}{2} \sigma_\beta^2 \right) \quad (2.35)$$

$$\hat{b}^3 = b_l^3 \exp \left(\frac{9}{2} \sigma_\beta^2 \right) = \overline{b^3}. \quad (2.36)$$

The right side of (2.36) is merely the arithmetic mean of b^3 , which is what *Neuzil and Tracy* (1981) found. When $\alpha = \pi/2$ and $\rho \rightarrow \infty$, we have the other quasi-two-dimensional model, and

$$\hat{b}^3 = b_l^3 \exp \left(-\frac{9}{2} \sigma_\beta^2 \right) = (\overline{b^{-3}})^{-1} \quad (2.37)$$

which is the harmonic mean of b^3 . All of these results are also found in the porous medium literature (*Gelhar and Axness*, 1983).

What is the expected value of Q_2 ? In general, it is non-zero:

$$\overline{Q_2} = \overline{bu_2} = -\frac{b_l^3 g J}{12\nu} \overline{3\beta \frac{\partial h}{\partial x_2}}. \quad (2.38)$$

Again, for any of the four spectra in Appendix A,

$$\overline{\beta \frac{\partial h}{\partial x_2}} = 3J\sigma_\beta^2 \left[\left(\frac{1-\rho}{1+\rho} \right) \sin \alpha \cos \alpha \right], \quad (2.39)$$

so that

$$\overline{Q}_2 = \frac{b_\ell^3 g J}{12\nu} \left[9\sigma_\beta^2 \left(\frac{\rho - 1}{\rho + 1} \right) \sin \alpha \cos \alpha \right]. \quad (2.40)$$

The cube of the effective aperture is thus, in general, a tensor. While we expect this in analogy with porous medium models, it has not been recognized to date in the fracture flow literature.

To generalize the results to a system where the mean gradient has arbitrary orientation:

$$\overline{Q}_i = \frac{b_\ell^3 g}{12\nu} \left[\left(1 + \frac{9}{2}\sigma_\beta^2 \right) \delta_{ij} - 9B_{ij} \right] J_j, \quad (2.41)$$

where δ_{ij} is the Kronecker delta, and

$$B_{ij} = \int_{\mathbf{k}} \frac{k_i k_j}{k^2} S_{\beta\beta}(k_1, k_2) dk_1 dk_2. \quad (2.42)$$

For the exponential spectrum,

$$B_{11} = \sigma_\beta^2 \left(\frac{\rho \sin^2 \alpha + \cos^2 \alpha}{\rho + 1} \right), \quad (2.43)$$

$$B_{22} = \sigma_\beta^2 \left(\frac{\rho \cos^2 \alpha + \sin^2 \alpha}{\rho + 1} \right), \quad (2.44)$$

$$B_{12} = B_{21} = -\sigma_\beta^2 \left(\frac{\rho - 1}{\rho + 1} \right) \sin \alpha \cos \alpha, \quad (2.45)$$

and thus the components of the effective aperture cubed tensor are

$$(\hat{b}^3)_{11} = b_\ell^3 \left\{ 1 + \sigma_\beta^2 \left[\frac{9}{2} - 9 \left(\frac{\rho \sin^2 \alpha + \cos^2 \alpha}{\rho + 1} \right) \right] \right\}, \quad (2.46)$$

$$(\hat{b}^3)_{22} = b_\ell^3 \left\{ 1 + \sigma_\beta^2 \left[\frac{9}{2} - 9 \left(\frac{\rho \cos^2 \alpha + \sin^2 \alpha}{\rho + 1} \right) \right] \right\}, \quad (2.47)$$

$$(\hat{b}^3)_{12} = (\hat{b}^3)_{21} = 9b_\ell^3 \sigma_\beta^2 \left(\frac{\rho - 1}{\rho + 1} \right) \sin \alpha \cos \alpha. \quad (2.48)$$

The principal directions of this tensor are α and $\alpha + \pi/2$. The principal values are

$$b_\ell^3 \left[1 + \frac{9}{2} \sigma_\beta^2 \left(\frac{\rho - 1}{\rho + 1} \right) \right] \cong b_\ell^3 \exp \left[\frac{9}{2} \sigma_\beta^2 \left(\frac{\rho - 1}{\rho + 1} \right) \right] \quad (2.49)$$

and

$$b_\ell^3 \left[1 - \frac{9}{2} \sigma_\beta^2 \left(\frac{\rho - 1}{\rho + 1} \right) \right] \cong b_\ell^3 \exp \left[-\frac{9}{2} \sigma_\beta^2 \left(\frac{\rho - 1}{\rho + 1} \right) \right] \quad (2.50)$$

The exponential generalization hypothesized in (2.49) and (2.50), which was proposed by *Gelhar and Arness* (1983), is exact for $\rho = 0$ and $\rho \rightarrow \infty$ (see (2.36) and (2.37)). The anisotropy ratio, R , is (2.49) divided by (2.50):

$$R = \exp \left[9 \sigma_\beta^2 \left(\frac{\rho - 1}{\rho + 1} \right) \right]. \quad (2.51)$$

Note that for an isotropic input covariance, $R = 1$, and the effective aperture becomes a scalar.

2.3. Effective aperture for velocity

The effective parallel-plate aperture which computes the same fluid velocity as the mean for our random-aperture model is slightly different from the one for fluid flux. This is essentially due to the fact that

$$\overline{b^3} \neq \overline{b} \overline{b^2}. \quad (2.52)$$

The method is the same, though. The mean velocity is given by taking the expected value of (2.4):

$$\overline{u_i} = \frac{b_\ell^2 g}{12\nu} \left[(1 + 2\sigma_\beta^2) \delta_{ij} - 6B_{ij} \right] J_j, \quad (2.53)$$

The components of the effective aperture squared tensor are thus:

$$\left(\hat{b}^2 \right)_{11} = b_\ell^2 \left\{ 1 + \sigma_\beta^2 \left[2 - 6 \left(\frac{\rho \sin^2 \alpha + \cos^2 \alpha}{\rho + 1} \right) \right] \right\} \quad (2.54)$$

$$(\hat{b}^2)_{22} = b_\ell^2 \left\{ 1 + \sigma_\beta^2 \left[2 - 6 \left(\frac{\rho \cos^2 \alpha + \sin^2 \alpha}{\rho + 1} \right) \right] \right\} \quad (2.55)$$

$$(\hat{b}^2)_{12} = (\hat{b}^2)_{21} = b_\ell^2 \left[6\sigma_\beta^2 \left(\frac{\rho - 1}{\rho + 1} \right) \sin \alpha \cos \alpha \right]. \quad (2.56)$$

With the definitions

$$\psi_{11} \equiv 2 - 6 \left(\frac{\rho \sin^2 \alpha + \cos^2 \alpha}{\rho + 1} \right) \quad (2.57)$$

$$\psi_{22} \equiv 2 - 6 \left(\frac{\rho \cos^2 \alpha + \sin^2 \alpha}{\rho + 1} \right) \quad (2.58)$$

$$\psi_{12} = \psi_{21} \equiv 6 \left(\frac{\rho - 1}{\rho + 1} \right) \sin \alpha \cos \alpha, \quad (2.59)$$

this can be written simply as

$$(\hat{b}^2)_{ij} = b_\ell^2 (\delta_{ij} + \sigma_\beta^2 \psi_{ij}). \quad (2.60)$$

This is also a tensor. It has the same principal directions as the effective aperture for flux. The principal values are

$$b_\ell^2 \left[1 + 2\sigma_\beta^2 \left(\frac{\rho - 2}{\rho + 1} \right) \right] \cong b_\ell^2 \exp \left[2\sigma_\beta^2 \left(\frac{\rho - 2}{\rho + 1} \right) \right] \quad (2.61)$$

and

$$b_\ell^2 \left[1 - 2\sigma_\beta^2 \left(\frac{2\rho - 1}{\rho + 1} \right) \right] \cong b_\ell^2 \exp \left[-2\sigma_\beta^2 \left(\frac{2\rho - 1}{\rho + 1} \right) \right] \quad (2.62)$$

and the anisotropy ratio is

$$R = \exp \left[6\sigma_\beta^2 \left(\frac{\rho - 1}{\rho + 1} \right) \right]. \quad (2.63)$$

All of the differences between the two effective apertures arise from the linearization of a cubic (flux) dependence on the aperture as opposed to that of a square (velocity) dependence. Some of the implications of these differences will be discussed in chapter 4.

Chapter 3.

Solute Transport

In this chapter, the effect of aperture variation on mass transport is investigated. In particular, the effect of the random variations in velocity produced by the random aperture model is evaluated. We expect, in analogy with *Gelhar and Axness (1983)*, to find that the mean concentration distribution will, after a sufficient time, and in the limit of zero or negligible local dispersion, be describable by a combination of effective advective and dispersive transport components. This result is achieved, albeit by a circuitous and seemingly unintuitive route.

The method is the same as in the previous chapter. First, an equation governing local relationships is assumed. The parameters and variables are written as stochastic processes, and the mean behavior of the governing equation is investigated. This involves evaluating certain cross-covariances, which turn out, as before, to be equivalent to effective homogeneous-parameter components of the mean of the governing equation.

In order to evaluate the effects of large-scale velocity variations on mass transport, two models of local mass transport are used. The first includes advection and a constant local Taylor dispersion due to the cross-sectional averaging of the parabolic velocity distribution. The local dispersion is eventually neglected, but its form has an effect on the results, producing physically unrealistic behavior. To get around this, a second model is discussed, which includes advection and a first-order decay, but no local dispersive component. The decay is also eventually neglected, but in this case, with no deleterious

mathematical artifacts. These two models are discussed in the next two sections.

3.1. Dispersive Model

The most intuitive model of local transport is the two-dimensional advection-dispersion model. The simplest version of this, and the one analyzed here, has a constant local dispersion coefficient, with Taylor dispersion plus molecular diffusion in the longitudinal direction and only diffusion in the transverse direction:

$$E_{11} \equiv D_L \equiv E + D_m, \quad (3.1)$$

$$E_{22} \equiv D_m, \quad (3.2)$$

$$E_{12} = E_{21} = 0. \quad (3.3)$$

For convenience, the x_1 -axis has been realigned with the direction of the mean velocity so that $\bar{u}_2 = 0$ and $\bar{u}_1 \equiv u$ (Figure 3.1).

There may be visualised two immediate objections to the reality of this model. First, since the Taylor dispersion coefficient for a parallel-plate fracture depends heavily on the aperture, a variable dispersion coefficient seems more realistic. The constant coefficient was selected for three reasons. First, it is simpler. Second, it enables clearer comparisons with the stochastic porous medium models. Third, *Naff* (1978) and *Gelhar et al.* (1979) found that for porous media, variations in dispersivity were not as important as velocity fluctuations in controlling macrodispersion.

The second objection to a constant dispersion coefficient lies in the fact that even for a constant-aperture fracture, the Taylor mechanism does not take effect immediately, but requires a certain amount of time for molecular diffusion to damp out any cross-sectional concentration gradients. Thus, if \mathbf{u} changes before this time, the Taylor mechanism cannot be said to have existed, and no constant, let alone Fickian, model will realistically represent the local mixing process.

Fischer et al. (1979) state that for a capillary tube, the longitudinal mass transport will be approximately Fickian for times t such

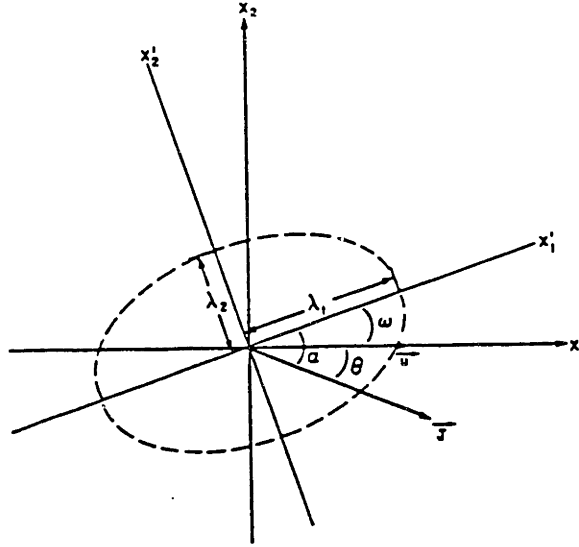


Figure 3.1: Orientation of correlation structure with respect to mean fluid velocity. Note that the x_1 direction is now with u , and not J .

that

$$t \geq \frac{2}{5} \frac{d^2}{D_m}. \quad (3.4)$$

Assume that this is true for parallel plates as well, with $b = d$. For a constant (cross-sectionally averaged) velocity u , a particle of water will travel a piston flow distance

$$x = ut \quad (3.5)$$

in this amount of time. Heuristically, the correlation scale, λ , of a process may be thought of as the distance over which that process is approximately constant. Then the Taylor mechanism will develop fully if the correlation scale, of a stochastic aperture is greater than the piston flow distance x . In other words, if

$$b^4 \leq \frac{30\lambda\nu D_m}{gJ}. \quad (3.6)$$

For the typical values:

$$D_m = 10^{-9} \text{ m.}^2/\text{s.}, \quad (3.7)$$

$$\nu = 10^{-6} \text{ m.}^2/\text{s.}, \quad (3.8)$$

$$\lambda = 1 \text{ m.}, \quad (3.9)$$

$$g = 10 \text{ m./s.}^2, \quad (3.10)$$

$$J = 10^{-2}, \quad (3.11)$$

b must be less than $750 \mu\text{m}$. This may be taken as an implicit assumption of the analysis in this section. In light of all of these observations, the assumption of a constant local dispersion coefficient seems acceptable.

Given this assumption, then the equation of conservation of mass for this cross-sectionally averaged system is

$$\frac{\partial}{\partial x_i} \left(bcu_i - bE_{ij} \frac{\partial c}{\partial x_j} \right) = 0. \quad (3.12)$$

Using the product rule for differentiation and the equation of continuity (2.6), we get

$$u_i \frac{\partial c}{\partial x_i} - E_{ij} \left(\frac{\partial(\ln b)}{\partial x_i} \frac{\partial c}{\partial x_j} + \frac{\partial^2 c}{\partial x_i \partial x_j} \right) = 0. \quad (3.13)$$

Substituting

$$\ln b = B + \beta(x_1, x_2) \quad (3.14)$$

$$c = \bar{c}(x_1, x_2) + c'(x_1, x_2) \quad (3.15)$$

$$u_i = \bar{u}_i + u'_i(x_1, x_2) \quad (3.16)$$

$$\bar{u}_1 \equiv u \neq 0 \quad (3.17)$$

$$\bar{u}_2 = 0, \quad (3.18)$$

taking the expected value gives us the mean equation

$$\bar{u}_i \frac{\partial \bar{c}}{\partial x_i} + \overline{u'_i \frac{\partial c'}{\partial x_i}} - E_{ij} \left(\frac{\partial \beta}{\partial x_i} \frac{\partial \bar{c}}{\partial x_j} + \frac{\partial^2 \bar{c}}{\partial x_i \partial x_j} \right) = 0. \quad (3.19)$$

The second and third terms represent additional solute fluxes due to the aperture variation. Each must be rewritten to avoid evaluating derivatives of c' , which would introduce unneeded mathematical complexities:

$$\overline{u'_i \frac{\partial c'}{\partial x_i}} = \frac{\partial}{\partial x_i} (\overline{u'_i c'}) - \overline{\frac{\partial u'_i}{\partial x_i} c'} \quad (3.20)$$

$$- E_{ij} \overline{\frac{\partial \beta}{\partial x_i} \frac{\partial c'}{\partial x_j}} = - \frac{\partial}{\partial x_i} \left(E_{ij} \overline{\frac{\partial \beta}{\partial x_j} c'} \right) + E_{ij} \overline{\frac{\partial^2 \beta}{\partial x_i \partial x_j} c'}. \quad (3.21)$$

These can be rearranged as

$$\frac{\partial}{\partial x_i} \left(\overline{u'_i c'} - E_{ij} \overline{\frac{\partial \beta}{\partial x_j} c'} \right) = \frac{\partial}{\partial x_i} \int_{\mathbf{k}} (S_{u,c}(\mathbf{k}) - ik_j E_{ij} S_{\beta c}(\mathbf{k})) d\mathbf{k} \quad (3.22)$$

$$- \overline{\frac{\partial u'_i}{\partial x_i} c'} + E_{ij} \overline{\frac{\partial^2 \beta}{\partial x_i \partial x_j} c'} = - \int_{\mathbf{k}} (ik_i S_{u,c}(\mathbf{k}) + k_i k_j E_{ij} S_{\beta c}(\mathbf{k})) d\mathbf{k}. \quad (3.23)$$

We hope to (and do) find that

$$\frac{\partial}{\partial x_i} \int_{\mathbf{k}} (S_{u,c}(\mathbf{k}) - ik_j E_{ij} S_{\beta c}(\mathbf{k})) d\mathbf{k} = - \frac{\partial}{\partial x_i} D_{ij} \frac{\partial \bar{c}}{\partial x_j}, \quad (3.24)$$

and

$$- \int_{\mathbf{k}} (ik_i S_{u,c}(\mathbf{k}) + k_i k_j E_{ij} S_{\beta c}(\mathbf{k})) d\mathbf{k} = - U_i \frac{\partial \bar{c}}{\partial x_i}, \quad (3.25)$$

where D_{ij} is the coefficient of macrodispersion and U_i is a correction to \bar{u}_i for finding the advective component of the mean solute flux. Thus, the mean equation will have the form

$$(\bar{u}_i - U_i) \frac{\partial \bar{c}}{\partial x_i} - (E_{ij} + D_{ij}) \frac{\partial^2 \bar{c}}{\partial x_i \partial x_j} = 0. \quad (3.26)$$

To evaluate these integrals, we need $S_{u,c}(\mathbf{k})$ and $S_{\beta c}(\mathbf{k})$ in terms of $S_{\beta\beta}(\mathbf{k})$. These transfer functions can be derived by looking at

the perturbation equation, which is found by subtracting (3.19) from (3.12) and neglecting terms like

$$a'b' - \overline{a'b'}.$$

This results in

$$\overline{u}_i \frac{\partial c'}{\partial x_i} + u'_i \frac{\partial \bar{c}}{\partial x_i} - E_{ij} \left(\frac{\partial \beta}{\partial x_i} \frac{\partial \bar{c}}{\partial x_j} + \frac{\partial^2 c'}{\partial x_i \partial x_j} \right) = 0. \quad (3.27)$$

Putting

$$G_i \equiv -\frac{\partial \bar{c}}{\partial x_i}, \quad (3.28)$$

and using the Fourier-Stieltjes representations (2.15) and (2.16) and

$$c' = \int_{\mathbf{k}} e^{i\mathbf{k}\cdot\mathbf{x}} dZ_c(\mathbf{k}), \quad (3.29)$$

we have

$$uik_1 dZ_c(\mathbf{k}) - G_i dZ_{u_i}(\mathbf{k}) + ig dZ_\beta(\mathbf{k}) + e dZ_c(\mathbf{k}) = 0. \quad (3.30)$$

where

$$g \equiv D_L k_1 G_1 + D_m k_2 G_2 \quad (3.31)$$

and

$$e \equiv D_L k_1^2 + D_m k_2^2. \quad (3.32)$$

The relationship between $dZ_\beta(\mathbf{k})$ and $dZ_{u_i}(\mathbf{k})$ can be derived from the perturbation form of the continuity equation:

$$\frac{\partial u'_i}{\partial x_i} + u \frac{\partial \beta}{\partial x_1} = 0, \quad (3.33)$$

giving

$$dZ_\beta(\mathbf{k}) = -\frac{k_i dZ_{u_i}(\mathbf{k})}{uk_1}. \quad (3.34)$$

Inserting (3.34) into (3.30) and solving for $dZ_c(\mathbf{k})$ yields

$$dZ_c(\mathbf{k}) = \left(\frac{uk_1 G_j + igk_j}{e + iuk_1} \right) \frac{dZ_{u_j}(\mathbf{k})}{uk_1}, \quad (3.35)$$

$$dZ_c^*(\mathbf{k}) = \left(\frac{uk_1 G_j - igk_j}{e - iuk_1} \right) \frac{dZ_{u_j}^*(\mathbf{k})}{uk_1}, \quad (3.36)$$

so that

$$S_{u,c}(\mathbf{k}) = \left(\frac{uk_1 G_j - igk_j}{e - iuk_1} \right) \frac{S_{u,u_j}(\mathbf{k})}{uk_1} \quad (3.37)$$

and, in real and imaginary parts,

$$S_{u,c}(\mathbf{k}) = \left[\frac{(uk_1 e G_j + uk_1 g k_j) + i(u^2 k_1^2 G_j - g e k_j)}{u^2 k_1^2 + e^2} \right] \frac{S_{u,u_j}(\mathbf{k})}{uk_1}. \quad (3.38)$$

To find $S_{u,u_j}(\mathbf{k})$ in terms of $S_{\beta\beta}(\mathbf{k})$, we investigate the perturbation form of (2.4):

$$u'_i = \gamma \left(2\beta J_i - \frac{\partial h}{\partial x_i} \right) \quad (3.39)$$

$$dZ_{u_i}(\mathbf{k}) = 2\gamma J_i dZ_{\beta}(\mathbf{k}) - \gamma i k_i dZ_h(\mathbf{k}), \quad (3.40)$$

where

$$\gamma \equiv \frac{b_l^2 g}{12\nu} \quad (3.41)$$

The generalization of (2.19) for arbitrary direction of mean gradient is

$$dZ_h(\mathbf{k}) = -\frac{3ik_j J_j}{k^2} dZ_{\beta}(\mathbf{k}), \quad (3.42)$$

which means

$$dZ_{u_i}(\mathbf{k}) = \gamma \left[2\delta_{ik} - 3 \left(\frac{k_i k_k}{k^2} \right) \right] J_k dZ_{\beta}(\mathbf{k}), \quad (3.43)$$

and

$$S_{u,u_j}(\mathbf{k}) = \gamma^2 \left[2\delta_{ik} - 3 \left(\frac{k_i k_k}{k^2} \right) \right] \left[2\delta_{jl} - 3 \left(\frac{k_j k_l}{k^2} \right) \right] J_k J_l S_{\beta\beta}(\mathbf{k}). \quad (3.44)$$

This equation is very similar to equation (61) of *Gelhar and Azness* (1983), the only difference being the existence of factors of 2 and 3 in our system, once again resulting from the cubic law. We now have $S_{u,c}(\mathbf{k})$ in terms of $S_{\beta\beta}(\mathbf{k})$. Also,

$$S_{\beta c}(\mathbf{k})d\mathbf{k} = \overline{dZ_{\beta}(\mathbf{k})dZ_c^*(\mathbf{k})}, \quad (3.45)$$

and using (3.34), we get

$$S_{\beta c}(\mathbf{k}) = -\frac{k_i}{uk_1}S_{u,c}(\mathbf{k}), \quad (3.46)$$

which gives us $S_{\beta c}(\mathbf{k})$ in terms of $S_{u,c}(\mathbf{k})$ and thus $S_{\beta\beta}(\mathbf{k})$.

The simplest input covariance is the isotropic exponential, which has the spectrum used here to evaluate (3.24). The integration involves extensive manipulations, with much use being made of the fact that integrals from $-\infty$ to ∞ of odd functions are zero (this removes the imaginary terms). Also, since the covariance is isotropic, $J_2 = 0$ simplifies matters. For

$$\epsilon \equiv \frac{D_L}{u\lambda} \quad (3.47)$$

much less than unity, integrals of the form

$$\int_{\mathbf{k}} \frac{S_{\beta\beta}(\mathbf{k})P(\mathbf{k})d\mathbf{k}}{u^2k_1^2 + (D_Lk_1^2 + D_mk_2^2)^2}$$

where $P(\mathbf{k})$ is a polynomial in k_1 and k_2 , may be approximated by noting that the main contribution will come from the area around $k_1 = 0$, rescaling the k_1 -axis as

$$k_1 = \epsilon z, \quad (3.48)$$

and taking $\epsilon \rightarrow 0$. This is equivalent to neglecting local dispersion.

For these approximations, and with the isotropic spectrum, we find that (see Appendix B.1)

$$D_{11} = \frac{4\gamma^2 J^2 \sigma_{\beta}^2 \lambda}{u} \quad (3.49)$$

and

$$D_{12} = D_{21} = D_{22} = 0. \quad (3.50)$$

Using (2.54), (3.49) may be rewritten

$$D_{11} = \frac{4u\sigma_\beta^2\lambda}{(1-\sigma_\beta^2)^2} \cong 4u\lambda\sigma_\beta^2 \exp(2\sigma_\beta^2), \quad (3.51)$$

which is interesting in that it is proportional to u . Thus, the longitudinal macrodispersivity exists and is proportional to λ and increases rapidly with σ_β^2 .

The evaluation of U_i does not require any approximation for an isotropic logaperture spectrum (see Appendix B.1). Here, $U_2 = 0$ and U_1 is given by

$$U_1 = \frac{\gamma^2 J^2 \sigma_\beta^2}{2u} = \frac{\sigma_\beta^2 u}{2(1-\sigma_\beta^2)^2} \cong \frac{1}{2} u \sigma_\beta^2 \exp(2\sigma_\beta^2). \quad (3.52)$$

This means that the effective velocity of solute advection is equal to

$$\hat{u} = u \left(1 - \frac{1}{2} \sigma_\beta^2 \exp(2\sigma_\beta^2) \right), \quad (3.53)$$

although it must be greater than zero.

When the input spectrum is anisotropic, as in Figure 3.1, however, problems arise. Previously, the term involving $S_{\beta c}(\mathbf{k})$ in (3.24) did not contribute to (3.49). In this case, this term behaves strangely, producing a non-symmetric D_{ij} and a divergent value of D_{22} . (See Appendix B.2 for these calculations.) An infinite cross-covariance is non-stationary. It is unclear whether this is due to mathematical artifact, is inherent in the assumption of constant E_{ij} , is due to the attempt to fit a Fickian local dispersion to our system or derives from the cross-sectional averaging. Fortunately, asymptotic macrodispersion coefficients can be found for an anisotropic input spectrum if a trick involving using decay in the local mass conservation equation is employed.

3.2. Decay model

In this model, the mass conservation equation is

$$\frac{\partial}{\partial x_i}(bu_i c) + bKc = 0, \quad (3.54)$$

where K is the decay constant. Using the equation of continuity, this becomes

$$u_i \frac{\partial c}{\partial x_i} + Kc = 0. \quad (3.55)$$

Note that b does not enter into the equation.

The mean of this is

$$\overline{u_i} \frac{\partial \bar{c}}{\partial x_i} + \overline{u_i' \frac{\partial c'}{\partial x_i}} + K\bar{c} = 0. \quad (3.56)$$

As before, we eliminate the derivative of c' :

$$\overline{u_i' \frac{\partial c'}{\partial x_i}} = \frac{\partial}{\partial x_i} \overline{u_i' c'} - \frac{\partial \overline{u_i' c'}}{\partial x_i} \quad (3.57)$$

and look for

$$\frac{\partial}{\partial x_i} \overline{u_i' c'} = -\frac{\partial}{\partial x_i} D_{ij} \frac{\partial \bar{c}}{\partial x_j} \quad (3.58)$$

and

$$-\frac{\partial \overline{u_i' c'}}{\partial x_i} = -U_i \frac{\partial \bar{c}}{\partial x_i}. \quad (3.59)$$

To evaluate D_{ij} , we again study the perturbation equation

$$\overline{u_i} \frac{\partial c'}{\partial x_i} + u_i' \frac{\partial \bar{c}}{\partial x_i} + Kc' = 0, \quad (3.60)$$

which gives

$$dZ_c(\mathbf{k}) = \frac{G_j}{K + iuk_1} dZ_{u_j}(\mathbf{k}) \quad (3.61)$$

$$S_{u,c}(\mathbf{k}) = \frac{K + iuk_1}{u^2k_1^2 + K^2} G_j S_{u,u}(\mathbf{k}) \quad (3.62)$$

Thus,

$$\overline{u'_i c'} = \int_{\mathbf{k}} S_{u,c}(\mathbf{k}) d\mathbf{k} = \int_{\mathbf{k}} \frac{K + iuk_1}{u^2k_1^2 + K^2} G_j S_{u,u}(\mathbf{k}) d\mathbf{k}, \quad (3.63)$$

and since $S_{u,u}(\mathbf{k})$ is unchanged, and is even in \mathbf{k} , the imaginary term drops out. D_{ij} is the part proportional to G_j . Now, the small parameter ϵ is

$$\epsilon \equiv \frac{K\lambda_1}{u}, \quad (3.64)$$

and after rescaling k_1 and taking $\epsilon \rightarrow 0$, the results for D_{ij} and U_i with an isotropic $S_{\beta\beta}(\mathbf{k})$ are the same as (3.49), (3.50) and (3.52) (see Appendix B.3), but with an anisotropic $S_{\beta\beta}(\mathbf{k})$, we get (see Appendix B.4)

$$D_{11} = \frac{4\sigma_\beta^2 \lambda_1 \gamma^2 J_1^2}{u(\rho^2 \sin^2 \omega + \cos^2 \omega)^{1/2}}, \quad (3.65)$$

$$D_{12} = D_{21} = -\frac{2\sigma_\beta^2 \lambda_1 \gamma^2 J_1 J_2}{u(\rho^2 \sin^2 \omega + \cos^2 \omega)^{1/2}}. \quad (3.66)$$

$$D_{22} = \frac{\sigma_\beta^2 \lambda_1 \gamma^2 J_2^2}{u(\rho^2 \sin^2 \omega + \cos^2 \omega)^{1/2}}, \quad (3.67)$$

Now, referring to Figure 3.2, with \tilde{u}_1 the component of \mathbf{u} in the direction of \mathbf{J} and \tilde{u}_2 is the component perpendicular to \mathbf{J} , we have, using (2.60) for $i = j = 1$,

$$u \cos \theta = \tilde{u}_1 = \gamma J (1 + \sigma_\beta^2 \psi_{11}) \quad (3.68)$$

and

$$u \sin \theta = \tilde{u}_2 = \gamma J (\sigma_\beta^2 \psi_{12}), \quad (3.69)$$

so that

$$J_1 = J \cos \theta = \frac{u \cos^2 \theta}{\gamma (1 + \sigma_\beta^2 \psi_{11})}, \quad (3.70)$$

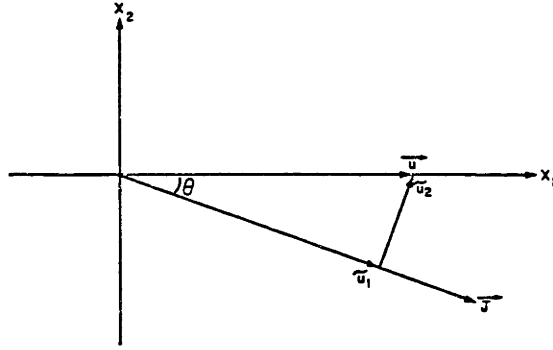


Figure 3.2: Definition of \tilde{u}_i .

and

$$J_2 = J \sin \theta = \frac{u \cos \theta \sin \theta}{\gamma (1 + \sigma_\beta^2 \psi_{11})}. \quad (3.71)$$

Thus,

$$D_{11} = \frac{4u\sigma_\beta^2\lambda_1 \cos^4 \theta}{(1 + \sigma_\beta^2 \psi_{11})^2 (\rho^2 \sin^2 \omega + \cos^2 \omega)^{1/2}}, \quad (3.72)$$

$$D_{12} = D_{21} = -\frac{2u\sigma_\beta^2\lambda_1 \cos^3 \theta \sin \theta}{(1 + \sigma_\beta^2 \psi_{11})^2 (\rho^2 \sin^2 \omega + \cos^2 \omega)^{1/2}}, \quad (3.73)$$

$$D_{22} = \frac{u\sigma_\beta^2\lambda_1 \cos^2 \theta \sin^2 \theta}{(1 + \sigma_\beta^2 \psi_{11})^2 (\rho^2 \sin^2 \omega + \cos^2 \omega)^{1/2}}. \quad (3.74)$$

The angles θ and ω are related to α by

$$\theta = \arctan \frac{\tilde{u}_2}{\tilde{u}_1} = \arctan \left\{ \frac{\sigma_\beta^2 \psi_{12}}{1 + \sigma_\beta^2 \psi_{11}} \right\} \quad (3.75)$$

and

$$\omega = \alpha - \theta. \quad (3.76)$$

Note that D_{12} and D_{21} are non-zero, which is not found for two-dimensional porous medium stochastic models (see (73) of *Gelhar and Arness, 1983*). This is due to the factors of 2 and 3 in $S_{u,u}(\mathbf{k})$ noted earlier.

The advection correction from (3.57) is found using the same method. The results are found in Appendix B.4 to be

$$U_1 = -\frac{u\sigma_\beta^2 \cos^2 \theta}{(1 + \sigma_\beta^2 \psi_{11})^2} \left\{ \frac{\rho [(\sin^2 \omega - 2 \cos^2 \omega) \cos^2 \theta + 3 \cos^2 \omega \sin^2 \theta]}{\rho + 1} + \frac{[(\cos^2 \omega - 2 \sin^2 \omega) \cos^2 \theta + 3 \sin^2 \omega \sin^2 \theta]}{\rho + 1} \right\} \quad (3.77)$$

$$U_2 = -\frac{2u\sigma_\beta^2 \cos^3 \theta \sin \theta}{(1 + \sigma_\beta^2 \psi_{11})^2} \times \left\{ \frac{\rho (2 \cos^2 \omega - \sin^2 \omega) + (2 \sin^2 \omega - \cos^2 \omega)}{\rho + 1} \right\}. \quad (3.78)$$

The significant feature here is that, since $U_2 \neq 0$, the effective direction of solute advection is not the same direction as \bar{u}_i , unless the logaperture process is isotropic, when the same results are obtained as for the dispersive model.

Chapter 4.

Summary and Discussion

A variable-aperture rock fracture is modeled as a two-dimensional stationary lognormal stochastic process. All quantities are averaged across this variable cross-section. This variation affects both flow and mass transport in the fracture as a coefficient in the two respective partial differential equations.

Equivalent homogeneous apertures are found which predict the same fluid velocity or flux as the areal mean velocity or flux for the random model. These effective apertures are dependent on the geometric mean, variance and correlation structure of the logaperture process. The cube of the effective aperture for flux and the square of the effective aperture for velocity are, in general, different tensors. The principal directions of these tensors are aligned with the directions of maximum and minimum correlation and thus when the logaperture process is statistically isotropic the effective apertures become scalars.

Mass transport is analyzed for the special case of zero local dispersion. Again, effective homogeneous dispersion coefficients and advection velocities due to the two-dimensional velocity variation are calculated for an advection-dispersion model of the transport of an areal mean concentration. This mean concentration must in general be neither constant nor planar. Thus, the areal average must be something like an areal moving average on a scale dependent on some Representative Elementary Area for concentration. A Fickian model for the local dispersion of the total concentration (mean plus perturbation) is assumed, with a constant dispersion coefficient. Even though this

dispersion is later neglected, its form and the cross-sectional averaging have an effect on the form of the resulting equivalent dispersion coefficients. When the logaperture process is isotropic, the longitudinal dispersion coefficient exists and is convectively controlled and the transverse coefficient is zero. However, when the logaperture process is anisotropic, the resulting dispersion matrix is asymmetric and divergent in the transverse direction. The physical significance of this is questionable. Since the resulting dispersion coefficient represents the effect only of the large-scale variations in fluid velocity, a more physically realistic result may be obtained by considering a local model of transport including advection and first-order decay but not dispersion, and then neglecting decay. In this case, the same results are obtained for an isotropic logaperture process, and for an anisotropic logaperture process, the effective dispersion coefficient is asymptotically constant and tensorial. All components are proportional to the areal mean velocity, the maximum correlation scale and a function of the logaperture variance.

Both local models predict that the effective velocity of solute advection is proportional to but does not coincide with the areal mean velocity. For an isotropic logaperture process, the directions both coincide with the direction of the mean hydraulic gradient, but the solute is retarded with respect to the fluid velocity. When the process is anisotropic, the directions do not even coincide, but both components of the effective velocity are still proportional to the magnitude of the areal mean.

Note that (3.55) does not include b , since the decay term is a sink, and thus lies outside the divergence. Then, no terms involving $\partial\beta/\partial x_i$ will appear in the mean equation. This is what enabled the decay model to produce stationary, physically realistic results. The same results occur if the local conservation of mass equation is assumed to be

$$\frac{\partial}{\partial x_i} (bu_i c) - bE_{ij} \frac{\partial^2 c}{\partial x_i \partial x_j} = 0, \quad (4.1)$$

which neglects the effect of the aperture variation on the dispersive flux, but not on the advective flux. Then, using (2.6), this equation

becomes

$$u_i \frac{\partial c}{\partial x_i} - E_{ij} \frac{\partial^2 c}{\partial x_i \partial x_j} = 0. \quad (4.2)$$

This is very similar to equation (12) of *Gelhar and Axness (1983)*. In their three-dimensional porous medium system, no variations in porosity or averaging distance occur. It appears that a requirement for this stochastic method to “work” is that any averaging distance be constant or non-apparent. Of course, this was never noticed for the porous medium analyses, but it explains a bit of why the decay trick was needed for the fracture system.

The fracture model differs from the two-dimensional porous medium model in that the solute does not travel with the mean velocity and that, due to the local cubic law, the off-diagonal terms in the macrodispersion tensor are nonzero for an anisotropic logaperture autocovariance.

The results of the dispersive model may reflect an inadequacy of the matrix diffusion model for field applications. In the diffusive model presented in this paper, the cross-sectional averaging produced an asymptotically constant Taylor dispersion coefficient for large time and constant aperture. When an “equivalent dispersion coefficient” is calculated for a matrix diffusion system with a constant fracture dispersivity, the same type of cross-sectional averaging is implied. However, when the dispersive model in this paper was used with a variable aperture, the cross-sectional averaging produced an asymptotically divergent dispersion coefficient. Thus, in the field, where apertures are likely to be heterogeneous, the question of whether the matrix diffusion effect controls or whether it has an equivalent advection-dispersion model remains unanswered. On the other hand, the solute retardation may enhance the matrix diffusion effect, since it allows more time for mass to enter into the porous rock matrix from the fracture.

Several different velocity averagings are discussed in the analysis. The first, $u_i(x_1, x_2)$, is the cross-sectional average of the parabolic Poeusille distribution to obtain the quadratic relationship between the mean velocity and the point value of the aperture. The second, \bar{u}_i , is the (constant) areal mean of u_i , and the third, $\hat{u}_i = \bar{u}_i - U_i$, is

the effective velocity of solute advection. Therefore, effective parallel-plate apertures calculated in the field from packer tests versus tracer tests may not be equal. Even when the tensorial nature of the effective aperture is neglected, i.e., for an isotropic logaperture process, the packer test, measuring fluid flux, will find (see (2.34))

$$\hat{b}_{\text{flux}} = b_{\ell}, \quad (4.3)$$

but the tracer test will measure \hat{u}_i and thus find (see (2.54) for $\rho = 1$ and (3.52))

$$\hat{b}_{\text{tracer}} = b_{\ell} \left[(1 - \sigma_{\beta}^2) \left(1 - \frac{\sigma_{\beta}^2}{2(1 - \sigma_{\beta}^2)^2} \right) \right]^{1/2}, \quad (4.4)$$

which is smaller than b_{ℓ} .

Gustafsson and Klockars (1981) found that their calculations of effective apertures using these two methods in the field produced a flux aperture which was larger than the tracer aperture by a factor of twenty. This can be used to evaluate σ_{β}^2 for the fracture tested, giving

$$\sigma_{\beta}^2 \cong \frac{1}{2}. \quad (4.5)$$

They also found dispersivities on the order of 1 m. Using (3.51), and $\sigma_{\beta}^2 = \frac{1}{2}$, we get

$$\lambda \cong 0.2 \text{ m.}, \quad (4.6)$$

which seems reasonable. Note, however, that this data may come from a fracture zone of two or more discrete pathways, and thus represent an equivalent single-fracture stochastic approximation of a multi-fracture system.

Novakowski et. al. (1984) found little difference between flux and velocity determinations of the effective aperture, which would indicate a low variance, except that their dispersivity was very high, at 1.55 m. for a 10.6 m. interwell distance. It is possible that the logaperture variance is very large, which would explain the lack of agreement between our model and their data.

The result that, for an anisotropic logaperture process, $U_2 \neq 0$ may have some effect on the analysis of two-well tracer tests, where the mean velocity field is not uniform. More work is necessary in order to determine the magnitude of the effect. This may in turn yield a method of calculating such parameters of the stochastic analysis as σ_β^2 or ρ from breakthrough curves.

Grisak et. al. (1980) found that in the lab, the effective aperture for a fractured till calculated from flux measurements was $40\mu\text{m}$., whereas an effective aperture of $7\mu\text{m}$ was required to fit an advection-dispersion model to a breakthrough curve for the sample (Figure 1.6). This also gives a σ_β^2 of about 0.5. They used a dispersivity of 0.15 m., which gives

$$\lambda \cong 0.03 \text{ m.}, \quad (4.7)$$

which is about an order of magnitude smaller than the field value derived above from *Gustafsson and Klockars* (1981). However, the fractures are quite different in terms of both material and scale so that comparison is probably fruitless.

Neretnieks et. al. (1982) also ran laboratory column tests, finding a dispersivity, fluid velocity and effective aperture from breakthrough curves. The aperture is not calculated, however, from flux data. The fluxes are given for each test, but the magnitude of the gradient is not, so no estimate of σ_β^2 can be made this way. However, they did calculate a σ_β^2 from a model considering the combined effect of several independent channels of flow, each of constant aperture, within the single fracture in their column, giving

$$\sigma_\beta^2 \cong 10^{-2}, \quad (4.8)$$

which, for their dispersivity of 0.025 m., gives a correlation scale of

$$\lambda = 0.6 \text{ m.} \quad (4.9)$$

This seems too large for the size of the sample, which is probably due to the assumption of constant aperture in the direction of flow. This points out the need for careful laboratory and field tests in order to determine just when the effect of velocity variations plays an important role in flow and mass transport in real fractures.

The possible scale effect noted by *Witherspoon et. al.* (1979) for the asymptotic value of K_f for large stress gives another indication of the typical magnitude of the correlation scale. Their explanation was that the larger samples exhibit a greater asymptotic hydraulic conductivity because they sample more apertures from the tail of the aperture distribution. If this is true, then the assumption of ergodicity is probably not valid at that scale. The correlation scales must then be a significant fraction of the scale of the largest test, which was about 1 m.

The assumption of ergodicity is implicit in the use of a stochastic model of the aperture. *Lumley and Panofsky* (1964) have shown for a one-dimensional system that this is satisfied if the scale of the problem is much larger than the correlation scale of the stochastic variable. Then, a spatial average of one realization of the process may approximate an ensemble average of many realizations. Stationarity is also an important assumption, allowing the Fourier-Stieltjes representations of the perturbations. For a single fracture, it seems plausible that the mean, variance and correlation scale be constant, although, of course, they may vary from fracture to fracture.

The assumption of steady state may seem unusual. However, *Gelhar and Axness* (1983) have shown that for a three-dimensional porous medium the steady-state dispersivities are the same as the asymptotically long-time results for a transient analysis. The assumption of a Fickian transport relationship requires a considerable "start-up" time for the mean concentration gradients to become smooth, so that the assumption of large time seems reasonable.

Another important assumption was that the perturbations be small so their products may be neglected. In addition, several derivations required that σ_β^2 be "small." Just how robust the theory is with regard to this assumption may not be quantified until careful Monte Carlo simulations are done. Until then, caution must be exercised when applying these results to situations with large variance must be done with great care.

Appendix A.

Autocovariances and Spectra

Four autocovariance/spectrum pairs were chosen to represent the statistical properties of the logaperture process. The first is based on the exponential decline of correlation with lag. This exponential autocovariance function, $R_{\beta\beta}(\xi)$, is

$$R_{\beta\beta}(\xi) = \sigma_{\beta}^2 \exp[-(\xi/\lambda)], \quad (A.1)$$

where σ_{β}^2 is the variance of the logaperture process, and

$$\frac{\xi}{\lambda} = \left(\frac{\xi_1^2}{\lambda_1^2} + \frac{\xi_2^2}{\lambda_2^2} \right)^{1/2} \quad (A.2)$$

where λ_1 and λ_2 are the correlation scales in the directions of maximum and minimum correlations, respectively, and ξ_i is the component of the lag vector in the direction of λ_i . The spectrum, $S_{\beta\beta}(\mathbf{k})$, for this covariance is

$$S_{\beta\beta}(\mathbf{k}) = \frac{\sigma_{\beta}^2 \lambda_1 \lambda_2}{2\pi(1 + \lambda_1^2 k_1^2 + \lambda_2^2 k_2^2)^{3/2}}, \quad (A.3)$$

where $S_{\beta\beta}(\mathbf{k})$ and k_i are the components of the two-dimensional wave number vector in the directions λ_i . This pair of functions is attractive because of the simplicity of the exponential function, and in particular its monotonic decline in correlation with distance.

The Whittle spectrum, used by *Whittle* (1954) and *Mizell et al.* (1982), also has a monotonically declining autocovariance function.

The Whittle spectrum and autocovariance are

$$S_{\beta\beta}(\mathbf{k}) = \frac{\sigma_{\beta}^2 \eta^2 \lambda_1 \lambda_2}{\pi(\eta^2 + \lambda_1^2 k_1^2 + \lambda_2^2 k_2^2)^2}, \quad \eta = \frac{\pi}{2} \quad (\text{A.4})$$

and

$$R_{\beta\beta}(\xi) = \sigma_{\beta}^2 \left(\frac{\pi \xi}{2\lambda} \right) K_1 \left(\frac{\pi \xi}{2\lambda} \right) \quad (\text{A.5})$$

where K_1 is the first-order modified Bessel function.

The Whittle A and Whittle B spectra were proposed by *Mizell et. al.* (1982) in order to produce a finite potential head variance due to variations in the transmissivity of a confined aquifer. As is shown in chapter 2, these spectra are also necessary to get a finite head variance in the fracture model. The Whittle A and B spectra are, respectively,

$$S_{(A)\beta\beta}(\mathbf{k}) = \frac{2\sigma_{\beta}^2 \eta^2 \lambda_1 \lambda_2 (\lambda_1^2 k_1^2 + \lambda_2^2 k_2^2)}{\pi(\eta^2 + \lambda_1^2 k_1^2 + \lambda_2^2 k_2^2)^3}, \quad \eta = \frac{\pi}{4} \quad (\text{A.6})$$

and

$$S_{(B)\beta\beta}(\mathbf{k}) = \frac{3\sigma_{\beta}^2 \eta^2 \lambda_1 \lambda_2 (\lambda_1^2 k_1^2 + \lambda_2^2 k_2^2)^2}{\pi(\eta^2 + \lambda_1^2 k_1^2 + \lambda_2^2 k_2^2)^4}, \quad \eta = \frac{3\pi}{16} \quad (\text{A.7})$$

and their autocovariances are

$$R_{(A)\beta\beta}(\xi) = \sigma_{\beta}^2 \left[\left(\frac{\pi \xi}{4\lambda} \right) K_1 \left(\frac{\pi \xi}{4\lambda} \right) - \frac{1}{2} \left(\frac{\pi \xi}{4\lambda} \right)^2 K_0 \left(\frac{\pi \xi}{4\lambda} \right) \right] \quad (\text{A.8})$$

and

$$R_{(B)\beta\beta}(\xi) = \sigma_{\beta}^2 \left\{ \left[1 + \frac{1}{8} \left(\frac{3\pi \xi}{16\lambda} \right)^2 \right] \left(\frac{3\pi \xi}{16\lambda} \right) K_1 \left(\frac{3\pi \xi}{16\lambda} \right) - \left(\frac{3\pi \xi}{16\lambda} \right)^2 K_0 \left(\frac{3\pi \xi}{16\lambda} \right) \right\}. \quad (\text{A.9})$$

Here, K_0 is the zero-order modified Bessel function.

These four covariances are plotted in Figure 2.2 of the main text.

Appendix B.

Details of Calculations

B.1. Dispersive model with isotropic logaperture process

From (3.24), we see that

$$D_{ij}G_j = \int_{\mathbf{k}} (S_{u,c} - ik_j E_{ij} S_{\beta c}) d\mathbf{k}. \quad (B.1)$$

Using (3.46), (3.38) and (3.44), and for $i = 1$,

$$\begin{aligned} D_{1j}G_j &= \int_{\mathbf{k}} \left(\frac{(uk_1 e G_j + uk_1 g k_j) + i(u^2 k_1^2 G_j - e g k_j)}{uk_1(u^2 k_1^2 + e^2)} \right) \times \\ &\quad \left[\left(\frac{u + ik_1 D_L}{u} \right) S_{u_1 u_j}(\mathbf{k}) + \left(\frac{ik_2 D_L}{u} \right) S_{u_2 u_j}(\mathbf{k}) \right] d\mathbf{k} \\ &= \frac{\gamma^2}{u^2} \int_{\mathbf{k}} \frac{S_{\beta\beta}(\mathbf{k}) d\mathbf{k}}{k^4 k_1^2 (u^2 k_1^2 + e^2)} \times \end{aligned}$$

$$\begin{aligned} &\{ G_1 [(D_L^2 D_m J_2^2 k_1^2) k_2^8 + \\ &\quad (((2D_L^2 D_m + D_L^3) J_2^2 + D_L^2 D_m J_1^2) k_1^4 + \\ &\quad (4D_m u^2 J_1^2 k_1^2)) k_2^6 + \end{aligned}$$

$$\begin{aligned}
& \left(\left(D_L^2 D_m + 2D_L^3 \right) J_2^2 + \left(2D_L^2 D_m + D_L^3 \right) J_1^2 \right) k_1^6 + \\
& \left(9D_m J_2^2 + 4(D_L - D_m) J_1^2 \right) u^2 k_1^4 k_2^4 + \\
& \left(\left(D_L^3 J_2^2 + \left(D_L^2 D_m + 2D_L^3 \right) J_1^2 \right) k_1^8 + \right. \\
& \left. \left(9D_L J_2^2 + (D_m - 4D_L) J_1^2 \right) u^2 k_1^6 \right) k_2^2 + \\
& \left(D_L^3 J_1^2 k_1^{10} + D_L J_1^2 u^2 k_1^8 \right) \Big] + \\
G_2 & \left[J_1 J_2 \left(2D_L D_m^2 k_1^2 k_2^8 + \right. \right. \\
& \left. \left(4D_L D_m^2 + 2D_L^2 D_m \right) k_1^4 - 4D_m u^2 k_1^2 \right) k_2^6 + \\
& \left. \left(2D_L D_m^2 + 4D_L^2 D_m \right) k_1^6 + (16D_m - 6D_L) u^2 k_1^2 \right) k_2^4 + \\
& \left. \left(2D_L^2 D_m k_1^8 + (2D_m + 12D_L) u^2 k_1^6 \right) k_2^2 \right] \Big\}. \tag{B.2}
\end{aligned}$$

The part proportional to G_1 is D_{11} and the part proportional to G_2 is D_{12} . For an isotropic $S_{\beta\beta}(\mathbf{k})$, $J_2 = 0$ and $J_1 = J \neq 0$. Thus $D_{12} = 0$ and

$$\begin{aligned}
D_{11} &= \frac{\gamma^2 J^2}{u^2} \int_{\mathbf{k}} \frac{S_{\beta\beta}(\mathbf{k}) d\mathbf{k}}{k^4 (u^2 k_1^2 + e^2)} \left\{ \left[D_L^2 D_m k_1^2 + 4D_m u^2 \right] k_2^6 + \right. \\
& \left[\left(2D_L^2 D_m + D_L^3 \right) k_1^4 + 4(D_L - D_m) u^2 k_1^2 \right] k_2^4 + \\
& \left[\left(D_L^2 D_m + 2D_L^3 \right) k_1^6 + (D_m - 4D_L) u^2 k_1^4 \right] k_2^2 + \\
& \left. \left[D_L^3 k_1^8 + D_L u^2 k_1^6 \right] \right\}. \tag{B.3}
\end{aligned}$$

For

$$\epsilon \equiv \frac{D_L}{u\lambda}, \tag{B.4}$$

$$\zeta_i \equiv \lambda k_i \tag{B.5}$$

and

$$\kappa \equiv \frac{D_m}{D_L}, \tag{B.6}$$

equation (B.3) becomes

$$\begin{aligned}
D_{11} &= \frac{\gamma^2 J^2}{u\lambda} \int_{\zeta} \frac{S_{\beta\beta}(\zeta) d\zeta}{\zeta^4 (\zeta_1^2 + \epsilon^2 (\zeta_1^2 + \kappa \zeta_2^2)^2)} \times \\
& \left[(\epsilon^3 \kappa \zeta_1^2 + 4\epsilon\kappa) \zeta_2^6 + (\epsilon^3 (2\kappa + 1) \zeta_1^4 + 4\epsilon(1 - \kappa) \zeta_1^2) \zeta_2^4 + \right. \\
& \left. (\epsilon^3 (\kappa + 2) \zeta_1^6 + \epsilon(\kappa - 4) \zeta_1^4) \zeta_2^2 + \epsilon^3 \zeta_1^8 + \epsilon \zeta_1^6 \right]. \quad (B.7)
\end{aligned}$$

Putting $\zeta_1 = \epsilon z$ and letting $\epsilon \rightarrow 0$ gives

$$\begin{aligned}
D_{11} &= \frac{\gamma^2 J^2}{u\lambda} \int_z \int_{\zeta_2} \frac{4\kappa \zeta_2^2 S_{\beta\beta}(0, \zeta_2) dz d\zeta_2}{z^2 + \kappa^2 \zeta_2^4} \\
&= \frac{2\gamma^2 J^2 \sigma_{\beta}^2 \lambda}{\pi u} \int_z \int_{\zeta_2} \frac{\kappa \zeta_2^2 dz d\zeta_2}{(z^2 + \kappa^2 \zeta_2^4) (1 + \zeta_2^2)^{3/2}} \\
&= \frac{4\gamma^2 J^2 \sigma_{\beta}^2 \lambda}{u}, \quad (B.8)
\end{aligned}$$

which is (3.49) in the text.

For $i = 2$,

$$\begin{aligned}
D_{2j} G_j &= \int_{\mathbf{k}} (S_{u_2 c}(\mathbf{k}) - ik_2 D_m S_{\beta c}(\mathbf{k})) d\mathbf{k} \\
&= \frac{\gamma^2}{u^2} \int_{\mathbf{k}} \frac{S_{\beta\beta}(\mathbf{k}) d\mathbf{k}}{k^4 k_1^2 (u^2 k_1^2 + e^2)} \times \\
& \{ G_1 [J_1 J_2 ((2D_L D_m^2 k_1^2) k_2^8 + (4D_L D_m^2 + 2D_L^2 D_m) k_1^4 k_2^6 + \\
& \quad ((2D_L D_m^2 + 4D_L^2 D_m) k_1^6 + (12D_m + 2D_L) u^2 k_1^4) k_2^4 + \\
& \quad (2D_L^2 D_m k_1^8 + (16D_L - 6D_m) u^2 k_1^6) k_2^2 - 4D_L u^2 k_1^8)] + \\
& G_2 [(D_m^3 J_2^2) k_2^{10} + ((2D_m^3 + D_L D_m^2) J_2^2 + D_m^3 J_1^2) k_1^2 k_2^8 + \\
& \quad ((D_m^3 + 2D_L D_m^2) J_2^2 + (2D_m^3 + D_L D_m^2) J_1^2) k_1^4 +
\end{aligned}$$

$$\begin{aligned}
& (D_m J_2^2 u^2 k_1^2) k_2^6 + \\
& \left((D_L D_m^2 J_2^2 + (D_m^3 + 2D_L D_m^2) J_1^2) k_1^6 + \right. \\
& \quad \left. ((D_L - 4D_m) J_2^2 + 9D_m J_1^2) u^2 k_1^4 \right) k_2^4 + \\
& \left(D_L D_m^2 J_1^2 k_1^8 + (4(D_m - D_L) J_2^2 + 9D_L J_1^2) u^2 k_1^6 \right) k_2^2 + \\
& \left. (4D_L J_2^2 u^2 k_1^6) \right\}. \tag{B.9}
\end{aligned}$$

Now, D_{21} is the part proportional to G_1 and D_{22} is the part proportional to G_2 . For the isotropic logaperture spectrum, $J_2 = 0$ and $J_1 = J \neq 0$ so that $D_{21} = 0$ and

$$\begin{aligned}
D_{22} &= \frac{\gamma^2 J^2}{u^2} \int_{\mathbf{k}} \frac{S_{\beta\beta}(\mathbf{k}) d\mathbf{k}}{k^4 (u^2 k_1^2 + e^2)} \times \\
& \left[(D_m^3) k_2^8 + ((2D_m^3 + D_L D_m^2) k_1^2) k_2^6 + \right. \\
& \quad \left((D_m^3 + 2D_L D_m^2) k_1^4 + 9D_m u^2 k_1^2 \right) k_2^4 + \\
& \quad \left. (D_L D_m^2 k_1^6 + 9D_L k_1^4) k_2^2 \right]. \tag{B.10}
\end{aligned}$$

Again, using

$$\epsilon \equiv \frac{D_m}{u\lambda}, \tag{B.11}$$

$$\zeta_i \equiv \lambda k_i \tag{B.12}$$

and

$$\kappa \equiv \frac{D_m}{D_L} \tag{B.13}$$

gives

$$\begin{aligned}
D_{22} &= \frac{\gamma^2 J^2}{u\lambda} \int_{\zeta} \frac{S_{\beta\beta}(\zeta) d\zeta}{\zeta^4 (\zeta_1^2 + \epsilon^2 (\zeta_1^2 + \kappa \zeta_2^2)^2)} \left[\epsilon \left(9\kappa u^2 \zeta_1^2 \zeta_2^4 + 9u^2 \zeta_1^4 \zeta_2^2 \right) + \right. \\
& \quad \left. \epsilon^3 \left(\kappa^3 \zeta_2^8 + (2\kappa^3 + \kappa^2) \zeta_1^2 \zeta_2^6 + (\kappa^3 + 2\kappa^2) \zeta_1^4 \zeta_2^4 + \kappa^2 \zeta_1^6 \zeta_2^2 \right) \right], \tag{B.14}
\end{aligned}$$

and when we substitute $\zeta_1 = \epsilon z$ the numerator becomes $\mathcal{O}(\epsilon^4)$ and the denominator becomes $\mathcal{O}(\epsilon^2)$, so that when we take $\epsilon \rightarrow 0$, D_{22} vanishes, as reported in the text.

To evaluate U_i , we start with a form of (3.25):

$$U_i G_i = - \int_{\mathbf{k}} (ik_i S_{u,c}(\mathbf{k}) + k_i k_j E_{ij} S_{\beta c}(\mathbf{k})) d\mathbf{k}. \quad (B.15)$$

Using (3.46), (3.38) and (3.44), this becomes

$$U_i G_i = - \int_{\mathbf{k}} (ik_i S_{u,c}(\mathbf{k}) + k_i k_j E_{ij} S_{\beta c}(\mathbf{k})) d\mathbf{k}, \quad (B.16)$$

which becomes, after using (3.46), (3.38) and (3.44),

$$\begin{aligned} U_i G_i = & - \frac{\gamma^2}{u} \int_{\mathbf{k}} \frac{S_{\beta\beta}(\mathbf{k}) d\mathbf{k}}{k_1^2 k_2^2} \times \\ & \left\{ G_1 \left[(3J_2^2 - 2J_1^2) k_1^2 k_2^2 + J_1^2 k_1^4 \right] + \right. \\ & \left. G_2 \left[J_1 J_2 (k_1^2 k_2^2 - 2k_1^4) \right] \right\}. \end{aligned} \quad (B.17)$$

The part proportional to G_1 is U_1 and the part proportional to G_2 is U_2 . For an isotropic $S_{\beta\beta}(\mathbf{k})$, $J_2 = 0$, and so $U_2 = 0$ and for the exponential spectrum, U_1 is given by

$$U_1 = \frac{\gamma^2 J^2 \sigma_\beta^2 \lambda^2}{2\pi u} \int_{\mathbf{k}} \frac{(2k_1^2 k_2^2 - k_1^4) d\mathbf{k}}{k_1^2 k_2^2 (1 + \lambda^2 k^2)^{3/2}}, \quad (B.18)$$

which is evaluated routinely in polar coordinates, yielding

$$U_1 = \frac{\gamma^2 J^2 \sigma_\beta^2}{2u}. \quad (B.19)$$

This is (3.52) in the text.

B.2. Dispersive model with anisotropic logaperture process

When the logaperture process is anisotropic, then $J_2 \neq 0$, and the macrodispersion coefficient is more complicated. From (B.2), we see that

$$\begin{aligned}
D_{11} = & \frac{\gamma^2}{u^2} \int_{\mathbf{k}} \frac{S_{\beta\beta}(\mathbf{k}') d\mathbf{k}}{k^4(u^2 k_1^2 + e^2)} \left\{ [D_L^2 D_m J_2^2] k_2^8 + \right. \\
& [((2D_L^2 D_m + D_L^3) J_2^2 + D_L^2 D_m J_1^2) k_1^2 + 4D_m J_1^2 u^2] k_2^6 + \\
& [((D_L^2 D_m + 2D_L^3) J_2^2 + (2D_L^2 D_m + D_L^3) J_1^2) k_1^4 + \\
& (9D_m J_2^2 + 4(D_L - D_m) J_1^2) u^2 k_1^2] k_2^4 + \\
& [(D_L^3 J_2^2 + (D_L^2 D_m + 2D_L^3) J_1^2) k_1^6 + \\
& (9D_L J_2^2 + (D_m - 4D_L) J_1^2) u^2 k_1^4] k_2^2 + \\
& \left. [D_L^3 J_1^2 k_1^8 + D_L J_1^2 u^2 k_1^6] \right\}. \tag{B.20}
\end{aligned}$$

where \mathbf{k}' is the wave number vector in the directions parallel to and perpendicular to the direction of maximum correlation.

Now, we use

$$k'_1 = k_1 \cos \omega + k_2 \sin \omega \tag{B.21}$$

$$k'_2 = -k_1 \sin \omega + k_2 \cos \omega \tag{B.22}$$

and substitute

$$\epsilon = \frac{D_L}{u\lambda_1}, \tag{B.23}$$

$$\zeta_i = \lambda_i k_i, \tag{B.24}$$

$$\rho = \frac{\lambda_1}{\lambda_2}, \tag{B.25}$$

$$\hat{\zeta}_1 = \epsilon z, \tag{B.26}$$

and let $\epsilon \rightarrow 0$ to get

$$\begin{aligned}
D_{11} &= \frac{4\gamma^2 J_1^2 \rho^2 \kappa \sigma_\beta^2 \lambda_1}{2\pi u} \times \\
&\int_z \int_{\zeta_1} \frac{\zeta_2^2 dz d\zeta_2}{(z^2 + \rho^4 \kappa^2 \zeta_2^4) [1 + \zeta_2^2 (\rho^2 \sin^2 \omega + \cos^2 \omega)]^{3/2}} \\
&= \frac{4\gamma^2 J_1^2 \sigma_\beta^2 \lambda_1}{u (\rho^2 \sin^2 \omega + \cos^2 \omega)^{1/2}}. \tag{B.27}
\end{aligned}$$

Similarly,

$$\begin{aligned}
D_{12} &= \frac{\gamma^2 J_1 J_2}{u^2} \int_{\mathbf{k}} \frac{S_{\beta\beta}(\mathbf{k}') d\mathbf{k}}{k^4 (u^2 k_1^2 + e^2)} \times \\
&\{ [2D_L D_m^2] k_2^8 + [(4D_L D_m^2 + 2D_i^2 D_m) k_1^2 - 4D_m u^2] k_2^6 + \\
&[(2D_L D_m^2 + 4D_L^2 D_m) k_1^4 + (16D_m - 6D_L) u^2 k_1^2] k_2^4 + \\
&[2D_L^2 D_m k_1^6 + (2D_m + 12D_L) u^2 k_1^4] k_2^2 \}. \tag{B.28}
\end{aligned}$$

Using the same substitutions as for D_{11} , and also letting $\epsilon \rightarrow 0$, gives

$$\begin{aligned}
D_{12} &= -\frac{4\gamma^2 J_1 J_2 \rho^2 \kappa \sigma_\beta^2 \lambda_1}{2\pi u} \times \\
&\int_z \int_{\zeta_2} \frac{\zeta_2^2 dz d\zeta_2}{(z^2 + \kappa^2 \rho^4 \zeta_2^4) [1 + \zeta_2^2 (\rho^2 \sin^2 \omega + \cos^2 \omega)]^{3/2}}, \tag{B.29}
\end{aligned}$$

or,

$$D_{12} = \frac{-4\gamma^2 J_1 J_2 \sigma_\beta^2 \lambda_1}{u (\rho^2 \sin^2 \omega + \cos^2 \omega)^{1/2}}. \tag{B.30}$$

From (B.9) we see that

$$D_{21} = \frac{\gamma^2 J_1 J_2}{u^2} \int_{\mathbf{k}} \frac{S_{\beta\beta}(\mathbf{k}') d\mathbf{k}}{k^4 (u^2 k_1^2 + e^2)} \times$$

$$\begin{aligned}
& \{ [2D_L D_m^2] k_2^8 + [(4D_L D_m^2 + 2D_L^2 D_m) k_1^2] k_2^6 + \\
& \quad [(2D_L D_m^2 + 4D_L^2 D_m) k_1^4 + (12D_m + 2D_L) u^2 k_1^2] k_2^4 + \\
& \quad [2D_L^2 D_m k_1^6 + (16D_L - 6D_m) u^2 k_1^4] k_2^2 - 4D_L u^2 k_1^6 \}. \quad (B.31)
\end{aligned}$$

Inserting (B.21), (B.22), (B.23), (B.24), (B.25), (B.6) and (B.26), we get

$$\begin{aligned}
D_{21} &= \frac{\gamma^2 J_1 J_2}{\lambda_2 u} \int_z \int_{\zeta_2} \frac{S_{\beta\beta}(\epsilon z, \zeta_2) dz d\zeta_2}{\rho^4 \zeta_2^4 (z^2 + \kappa^2 \rho^4 \zeta_2^4)} \times \\
& \quad \left\{ \epsilon^2 [2\kappa^2 \rho^8 \zeta_2^8 + (12\kappa + 2) \rho^4 u^2 z^2 \zeta_2^4] + \mathcal{O}(\epsilon^4) \right\}, \quad (B.32)
\end{aligned}$$

so that when we take $\epsilon \rightarrow 0$, we get $D_{21} = 0$. Note that $D_{21} \neq D_{12}$, so that in this case, the dispersion coefficient is asymmetric.

Similarly, D_{22} is evaluated by using the same substitutions in (B.9) and letting $\epsilon \rightarrow 0$, finding that

$$D_{22} = \frac{\gamma^2 J_2^2}{u \lambda_2} \int_z \int_{\zeta_2} \frac{S_{\beta\beta}(0, \zeta_2) (\kappa^3 \rho^{10} \zeta_2^{10} + \kappa \rho^6 z^2 \zeta_2^6) dz d\zeta_2}{\rho^4 \zeta_2^4 z^2 (z^2 + \kappa^2 \rho^4 \zeta_2^4)}, \quad (B.33)$$

which integral in z diverges! This is nonstationary behavior.

U_1 and U_2 are evaluated using (B.17) for nonzero J_2 . Thus,

$$U_1 = -\frac{\gamma^2}{u} \int_{\mathbf{k}} \frac{S_{\beta\beta}(\mathbf{k}') d\mathbf{k}}{k^2 k_1^2} \left[(3J_2^2 - 2J_1^2) k_1^2 k_2^2 + J_1^2 k_1^4 \right]. \quad (B.34)$$

After using

$$k_1 = k_1' \cos \omega - k_2' \sin \omega \quad (B.35)$$

$$k_2 = k_1' \sin \omega + k_2' \cos \omega \quad (B.36)$$

to transform to the primed coordinate system, (B.34) can be integrated in polar coordinates to yield

$$U_1 = -\frac{\gamma^2 \sigma_\beta^2}{u} \left\{ \frac{\rho \left[(\sin^2 \omega - 2 \cos^2 \omega) J_1^2 + 3 \cos^2 \omega J_2^2 \right]}{\rho + 1} + \right.$$

$$\left. \frac{[(\cos^2 \omega - 2 \sin^2 \omega) J_1^2 + 3 \sin^2 \omega J_2^2]}{\rho + 1} \right\}. \quad (B.37)$$

Of course, $\gamma^2 J_1^2$ and $\gamma^2 J_2^2$ can be written in terms of u , $\cos \theta$ and $\sin \theta$ using (3.70) and (3.71).

Similarly,

$$U_2 = -\frac{\gamma^2}{u} \int_{\mathbf{k}} \frac{S_{\beta\beta}(\mathbf{k}') d\mathbf{k}}{k^2 k_1^2} [J_1 J_2 (k_1^2 k_2^2 - 2k_1^4)], \quad (B.38)$$

which is evaluated the same way as U_1 , giving

$$U_2 = \frac{\gamma^2 \sigma_\beta^2}{u} \left\{ \frac{\rho [(2 \sin^2 \omega - \cos^2 \omega) J_1 J_2]}{\rho + 1} + \frac{[(2 \cos^2 \omega - \sin^2 \omega) J_1 J_2]}{\rho + 1} \right\}. \quad (B.39)$$

B.3. Decay model with isotropic logaperture process

From (3.58) and (3.63), we see that

$$D_{ij} G_j = \int_{\mathbf{k}} \frac{K + iuk_1}{u^2 k_1^2 + K^2} G_j S_{u,u}(\mathbf{k}) d\mathbf{k}, \quad (B.40)$$

and using (3.44), we have

$$D_{ij} = \gamma^2 \int_{\mathbf{k}} \frac{(2k^2 \delta_{ik} - 3k_i k_k)(2k^2 \delta_{jl} - 3k_j k_l) J_k J_l K S_{\beta\beta}(\mathbf{k}) d\mathbf{k}}{k^4 (u^2 k_1^2 + K^2)}. \quad (B.41)$$

Thus,

$$D_{11} = \gamma^2 \int_{\mathbf{k}} \frac{[2k^2 J_1 - 3k_1 (k_l J_l)]^2 K S_{\beta\beta}(\mathbf{k}) d\mathbf{k}}{k^4 (u^2 k_1^2 + K^2)}, \quad (B.42)$$

$$D_{12} = D_{21} = -\gamma^2 J_1 J_2 \int_{\mathbf{k}} \frac{(2k_2^4 - 14k_1^2 k_2^2 + 2k_1^4) K S_{\beta\beta}(\mathbf{k}) d\mathbf{k}}{k^4 (u^2 k_1^2 + K^2)}, \quad (B.43)$$

and

$$D_{22} = -\gamma^2 \int_{\mathbf{k}} \frac{(4J_2^2 k_1^2 k_2^2 - J_2^2 k_2^4 - 9J_1^2 k_1^2 k_2^2 - 4J_2^2 k_1^4) K S_{\beta\beta}(\mathbf{k}) d\mathbf{k}}{k^4 (u^2 k_1^2 + K^2)}. \quad (B.44)$$

For an isotropic logaperture spectrum, $J_2 = 0$ and $J_1 = J \neq 0$, so that

$$D_{12} = D_{21} = 0, \quad (B.45)$$

and

$$D_{11} = \frac{\gamma^2 J^2 \lambda^2 \sigma_\beta^2}{2\pi} \int_{\mathbf{k}} \frac{(4k_2^4 - 4k_1^2 k_2^2 + k_1^4) K d\mathbf{k}}{k^4 (u^2 k_1^2 + K^2) (1 + \lambda^2 k^2)^{3/2}}. \quad (B.46)$$

Putting

$$K = \frac{\epsilon u}{\lambda}, \quad (B.47)$$

$$k_1 = \frac{\epsilon z}{\lambda} \quad (B.48)$$

and

$$k_2 = \frac{\zeta_2}{\lambda}, \quad (B.49)$$

and letting $\epsilon \rightarrow 0$ gives

$$\begin{aligned} D_{11} &= \frac{2\sigma_\beta^2 \gamma^2 J^2 \lambda^2}{\pi u} \int_z \int_{\zeta_2} \frac{dz d\zeta_2}{(1+z^2)(1+\zeta_2^2)^{3/2}} \\ &= \frac{4\sigma_\beta^2 \gamma^2 J^2 \lambda}{u} \end{aligned} \quad (B.50)$$

which is seen to be the same as for the dispersive model.

Note that D_{22} in (B.44) has a term proportional to J_1^2 , so that it does not automatically vanish for an isotropic logaperture spectrum. The remaining term is

$$D_{22} = 9\gamma^2 J^2 \int_{\mathbf{k}} \frac{k^2 k_1^2 K S_{\beta\beta}(\mathbf{k}) d\mathbf{k}}{k^4 (u^2 k_1^2 + K^2)}. \quad (B.51)$$

However, when using the substitutions (B.47), (B.48) and (B.49), we find that $D_{22} \sim O(\epsilon^2)$, and thus goes to zero.

From (3.59) and (3.62),

$$\begin{aligned} U_j G_j &= -\frac{\partial u'_i}{\partial x_i} c' = -\int_{\mathbf{k}} i k_i S_{u,c}(\mathbf{k}) d\mathbf{k}, \\ &= u \int_{\mathbf{k}} \frac{k_1 k_i G_j S_{u,u_j}(\mathbf{k}) d\mathbf{k}}{u^2 k_1^2 + K^2}. \end{aligned} \quad (B.52)$$

Thus, using (3.44)

$$U_1 = -\gamma^2 u \int_{\mathbf{k}} \frac{(3J_2^2 k_1^2 k_2^2 - 2J_1^2 k_1^2 k_2^2 + J_1^2 k_1^4) S_{\beta\beta}(\mathbf{k}) d\mathbf{k}}{k^2 (u^2 k_1^2 + K^2)} \quad (B.53)$$

and

$$U_2 = \gamma^2 J_1 J_2 u \int_{\mathbf{k}} \frac{(2k_1^4 - 4k_1^2 k_2^2) S_{\beta\beta}(\mathbf{k}) d\mathbf{k}}{k^2 (u^2 k_1^2 + K^2)}. \quad (B.54)$$

For $J_2 = 0$, $U_2 = 0$ and

$$U_1 = \frac{\gamma^2 J^2 \sigma_\beta^2 u \lambda^2}{2\pi} \int_{\mathbf{k}} \frac{(k_1^4 - 2k_1^2 k_2^2) d\mathbf{k}}{k^2 (u^2 k_1^2 + K^2) (1 + \lambda^2 k^2)^{3/2}}, \quad (B.55)$$

and with $\zeta_i = \lambda k_i$ and (B.47),

$$U_1 = \frac{\gamma^2 J^2 \sigma_\beta^2}{2\pi u} \int_{\zeta_1} \int_{\zeta_2} \frac{(2\zeta_2^2 - \zeta_1^2) d\zeta_1 d\zeta_2}{\zeta^2 (1 + \zeta^2)^{3/2}} = \frac{\gamma^2 J^2 \sigma_\beta^2}{2u} \quad (B.56)$$

B.4. Decay model with anisotropic logaperture process

When the logaperture process is anisotropic, J_2 is in general nonzero in (B.42), (B.43), (B.44), (B.53) and (B.54). Using (B.21) and (B.22) in (B.42), substituting

$$K = \frac{\epsilon u}{\lambda_1}, \quad (B.57)$$

$$k_1 = \frac{\epsilon z}{\lambda_1} \quad (B.58)$$

and

$$k_2 = \frac{\zeta_2}{\lambda_1}, \quad (B.59)$$

and letting $\epsilon \rightarrow 0$ gives

$$\begin{aligned} D_{11} &= \frac{4\gamma^2 J_1^2 \sigma_\beta^2 \lambda_1}{2\pi u} \int_z \int_{\zeta_2} \frac{dz d\zeta_2}{(1+z^2)(1+\zeta_2^2(\rho^2 \sin^2 \omega + \cos^2 \omega))^{3/2}} \\ &= \frac{4\gamma^2 J_1^2 \sigma_\beta^2 \lambda_1}{u(\rho^2 \sin^2 \omega + \cos^2 \omega)^{1/2}}, \end{aligned} \quad (B.60)$$

which is (3.65) in the text.

The same method applied to (B.43) shows that

$$\begin{aligned} D_{12} = D_{21} &= -\frac{\gamma^2 J_1 J_2 \sigma_\beta^2 \lambda_1}{\pi u} \times \\ &\int_z \int_{\zeta_2} \frac{dz d\zeta_2}{(1+z^2)(1+\zeta_2^2(\rho^2 \sin^2 \omega + \cos^2 \omega))^{3/2}} \\ &= -\frac{2\gamma^2 J_1 J_2 \sigma_\beta^2 \lambda_1}{u(\rho^2 \sin^2 \omega + \cos^2 \omega)^{1/2}}, \end{aligned} \quad (B.61)$$

which is (3.66) in the text.

Similarly, from (B.44), we see that

$$\begin{aligned} D_{22} &= \frac{\gamma^2 J_2^2 \sigma_\beta^2 \lambda_1}{2\pi u} \int_z \int_{\zeta_2} \frac{dz d\zeta_2}{(1+z^2)(1+\zeta_2^2(\rho^2 \sin^2 \omega + \cos^2 \omega))^{3/2}} \\ &= \frac{\gamma^2 J_2^2 \sigma_\beta^2 \lambda_1}{u(\rho^2 \sin^2 \omega + \cos^2 \omega)^{1/2}}, \end{aligned} \quad (B.62)$$

which is (3.67) in the text.

To find U_1 , start with (B.53) and transform to the primed coordinate system using (B.35) and (B.36) to get

$$U_1 = -\frac{\gamma^2 \sigma_\beta^2 \lambda_1 \lambda_2}{2\pi u} \int_{\mathbf{k}'} \frac{d\mathbf{k}'}{k'^2 (1 + \lambda_1^2 k_1'^2 + \lambda_2^2 k_2'^2)^{3/2}} \times$$

$$\left[J_1^2 \left(k_1'^2 (\cos^2 \omega - 2 \sin^2 \omega) + k_2'^2 (\sin^2 \omega - 2 \cos^2 \omega) \right) + \right.$$

$$\left. J_2^2 \left(3k_1'^2 \sin^2 \omega + 3k_2'^2 \cos^2 \omega \right) \right], \quad (\text{B.63})$$

which is routinely integrated to obtain

$$U_1 = -\frac{\gamma^2 \sigma_\beta^2}{u} \left\{ \frac{\rho \left[(\sin^2 \omega - 2 \cos^2 \omega) J_1^2 + 3 \cos^2 \omega J_2^2 \right]}{\rho + 1} + \right.$$

$$\left. \frac{\left[(\cos^2 \omega - 2 \sin^2 \omega) J_1^2 + 3 \sin^2 \omega J_2^2 \right]}{\rho + 1} \right\}. \quad (\text{B.64})$$

This is equivalent to (3.77).

To find U_2 , use (B.35) and (B.36) in (B.54) to get

$$U_2 = -\frac{\gamma^2 J_1 J_2 \sigma_\beta^2 \lambda_1 \lambda_2}{\pi u} \int_{\mathbf{k}'} \frac{d\mathbf{k}'}{k'^2 (1 + \lambda_1^2 k_1'^2 + \lambda_2^2 k_2'^2)^{3/2}} \times$$

$$\left[(2 \sin^2 \omega - \cos^2 \omega) k_1'^2 + (2 \cos^2 \omega - \sin^2 \omega) k_2'^2 \right]$$

$$= -\frac{2\gamma^2 J_1 J_2 \sigma_\beta^2}{u} \left\{ \frac{\rho \left(2 \cos^2 \omega - \sin^2 \omega \right) + \left(2 \sin^2 \omega - \cos^2 \omega \right)}{\rho + 1} \right\}, \quad (\text{B.65})$$

which is equivalent to (3.78) in the text.

Appendix C.

Bibliography

1. Barker, J. A., *Laplace Transform Solutions for Solute Transport in Fissured Aquifers*, **Adv. Wat. Res.**, 5, 98-104, 1982.
2. Barker, J. A., and S. D. Foster, *A Diffusion Exchange Model for Solute Movement in Fissured Porous Rock*, **Q. J. Eng. Geol. London**, 14, 17-24, 1981.
3. Bianchi, L., and D. T. Snow, *Permeability of Crystalline Rock Interpreted from Measured Orientations and Apertures of Fractures*, **Annals of the Arid Zone**, 8(2), 231-245, 1968.
4. Castillo, E., G. M. Karadi and R. J. Krizek, *Unconfined Flow through Jointed Rock*, **Wat. Res. Bull.**, 8(2), 266-281,
5. Elder, J. W., *The Dispersion of Marker Fluid in Turbulent Shear Flow*, **Journal of Fluid Mechanics**, 5, 544-560, 1965.
6. Erickson, K. L., *A Fundamental Approach to the Analysis of Radionuclide Transport Resulting from Fluid Flow through Jointed Porous Media*, Sandia National Laboratories report SAND80-0457, 1981.
7. Fischer, H. B., E. J. List, R. C. Y. Koh, J. Imberger and N. H. Brooks, *Mixing in Inland and Coastal Waters*, Academic Press, New York, 1979.
8. Gangi, A. F., *Variation of Whole and Fractured Porous Rock Permeability with Confining Pressure*, **Int. J. Rock Mech. Min. Sci. & Geomech. Abstr.**, 15, 249-257, 1978.

9. Gelhar, L. W., and C. L. Axness, *Three-Dimensional Stochastic Analysis of Macrodispersion in Aquifers*, *Wat. Res. Res.*, 19(1), 161-180, 1983.
10. Gelhar, L. W., A. L. Gutjahr, and R. L. Naff, *Stochastic Analysis of Macrodispersion in a Stratified Aquifer*, *Wat. Res. Res.*, 15(6), 1387-1397, 1979.
11. Gradshteyn, I. S., and I. M. Ryzhik, *Tables of Integrals, Series, and Products*, Academic Press, New York, 1980.
12. Grisak, G. E., personal communication, 1984.
13. Grisak, G. E., and J. F. Picketts, *Solute Transport through Fractured Media, 1. The Effect of Matrix Diffusion*, *Wat. Res. Res.*, 16(4), 719-730, 1980.
14. Grisak, G. E., and J. F. Picketts, *An Analytical Solution for Solute Transport through Fractured Media with Matrix Diffusion*, *J. Hydr.*, 52, 47-57, 1981.
15. Grisak, G. E., J. F. Picketts and J. A. Cherry, *Solute Transport through Fractured Media, 2. Column Study of Fractured Till*, *Wat. Res. Res.*, 16(4), 731-739, 1980.
16. Gustafsson, E., and C.-E. Klockars, *Studies on Groundwater Transport in Fractured Crystalline Rock under Controlled Conditions using Nonradioactive Tracers*, KBS technical report 81-07, 1981.
17. Huyakorn, P. S., B. H. Lester, and J. W. Mercer, *An Efficient Finite Element Technique for Modeling Transport in Fractured Porous Media, 1. Single Species Transport*, *Wat. Res. Res.*, 19(3), 841-854, 1983a.
18. Huyakorn, P. S., B. H. Lester, and J. W. Mercer, *An Efficient Finite Element Technique for Modeling Transport in Fractured Porous Media, 2. Nuclide Decay Chain Transport*, *Wat. Res. Res.*, 19(5), 1286-1296, 1983b.
19. Karadi, G. M., R. J. Krizek and E. Castillo, *Hydrodynamic Dispersion in a Single Rock Joint*, *J. Appl. Phys.*, 43(12), 5013-5021, 1972.

20. Kranz, R. L., A. D. Frankel, T. Engelder and C. H. Scholz, *The Permeability of Whole and Jointed Barre Granite*, **Int. J. Rock Mech. Min. Sci. & Geomech. Abstr.**, 16, 225-234, 1979.
21. Langlois, W. E., *Slow Viscous Flow*, The Macmillan Company, New York, 1964.
22. Louis, C., *A Study of Ground Water Flow in Jointed Rock and its Influence on the Stability of Rock Masses*, Rock Mechanics Report No. 10, Imperial College, London, 1969.
23. Lumley, J. L., and H. A. Panofsky, *The Structure of Atmospheric Turbulence*, John Wiley, New York, 1964.
24. Mizell, S. A., A. L. Gutjahr and L. W. Gelhar, *Stochastic Analysis of Spatial Variability in Two-Dimensional Steady Groundwater Flow Assuming Stationary and Non-Stationary Heads*, **Wat. Res. Res.**, 18(4), 1053-1067, 1982.
25. Naff, R. L., *A Continuum Approach to the study and Determination of Field Longitudinal Dispersion Coefficients*, Ph. D. dissertation, N. M. Inst. of Mining and Technol., Socorro, June, 1978.
26. Nelson, R., and J. Handin, *Experimental Study of Fracture Permeability in Porous Rock*, **Amer. Assoc. Petr. Geol. Bull.**, 61(2), 227-236, 1977.
27. Neretnieks, I., *Diffusion in the Rock Matrix: An Important Factor in Radionuclide Retardation?* **J. Geophys. Res.**, 85(B8), 4379-4397, 1980.
28. Neretnieks, I., *A Note on Fracture Flow Dispersion Mechanisms in the Ground*, **Wat. Res. Res.**, 19(2), 364-370, 1983.
29. Neretnieks, I., T. Eriksen and P. Tähtinen, *Tracer Movement in a Single Fissure in Granitic Rock: Some Experimental Results and Their Interpretation*, **Wat. Res. Res.**, 18(4), 849-858, 1982.
30. Neuzil, C. E., and J. V. Tracy, *Flow through Fractures*, **Wat. Res. Res.**, 17(1), 191-199, 1981.

31. Noorishad, J., and M. Mehran, *An Upstream Finite Element Method for Solution of the Transient Transport Equation in Fractured Porous Media*, *Wat. Res. Res.*, 18(3), 588-596, 1982.
32. Novakowski, K. S., P. A. Flavelle, K. G. Raven and E. L. Cooper, *Determination of Groundwater Flow Pathways in Fractured Plutonic Rock Using a Radioactive Tracer* submitted to *Int. J. Appl. Rad. and Isotopes*, 1984.
33. Pratt, H. R., H. S. Swolfs, W. F. Brace, A. D. Black and J. W. Handin, *Elastic and Transport Properties of an in situ Jointed Granite*, *Int. J. Rock Mech. Min. Sci. & Geomech. Abstr.*, 14, 35-45, 1977.
34. Rasmuson, A., T. N. Narasimhan and I. Neretnieks, *Chemical Transport in a Fissured Rock: Verification of a Numerical Model*, *Wat. Res. Res.*, 18(5), 1479-1492, 1982.
35. Rasmuson, A., and I. Neretnieks, *Migration of Radionuclides in Fissured Rock: The Influence of Micropore Diffusion and Longitudinal Dispersion*, *J. Geophys. Res.*, 86(B5), 3749-3758, 1981.
36. Rocha, M., and F. Franciss, *Determination of Permeability in Anisotropic Rock Masses from Integral Samples*, in *Structural and Geotechnical Mechanics*, J. W. Hall, ed., Prentice Hall, New York, 178-202, 1977.
37. Snow, D. T., *Three-Hole Pressure Test for Anisotropic Foundation Permeability*, *Felsmechanik und Ingenieurgeologie*, 4(4), 298-316, 1966.
38. Snow, D. T., *Rock Fracture Spacings, Openings and Porosities*, *J. Soil Mech. Found. Div., ASCE*, (SM1) 73-91, 1968a.
39. Snow, D. T., *Hydraulic Character of Fractured Metamorphic Rocks of the Front Range and Implications to the Rocky Mountain Arsenal Well*, *Colo. Sch. Min. Quart.*, 63(1), 1968b.
40. Snow, D. T., *Fracture Deformation and Changes of Permeability and Storage upon Changes of Fluid Pressure*, *Colo. Sch. Min. Quart.*, 63(1), 201-244, 1968c.

41. Snow, D. T., *Anisotropic Permeability of Fractured Media*, *Wat. Res. Res.*, 5(6), 1273-1289, 1969.
42. Snow, D. T., *The Frequency and Apertures of Fractures in Rock*, *Int. J. Rock Mech. Min. Sci.*, 7, 23-40, 1970.
43. Sudicky, E. A., and E. O. Frind, *Contaminant Transport in Fractured Porous Media: Analytical Solutions for a System of Parallel Fractures*, *Wat. Res. Res.*, 18(6), 1634-1642, 1982.
44. Sudicky, E. A., and E. O. Frind, *Contaminant Transport in Fractured Porous Media: Analytical Solution for a Two-Member Decay Chain in a Single Fracture*, *Wat. Res. Res.*, 20(7), 1021-1029, 1984.
45. Tang, D. H., E. O. Frind and E. A. Sudicky, *Contaminant Transport in Fractured Porous Media: Analytical Solution for a Single Fracture*, *Wat. Res. Res.*, 17(3), 555-564, 1981.
46. Taylor, G. I., *The Dispersion of Soluble Matter in Solvent Flowing Slowly through a Tube*, *Proc. R. Soc. London Ser. A*, 219, 189-203, 1953.
47. Uffink, G. J. M., *Dampening of Fluctuations in Groundwater Temperature by Heat Exchange Between the Aquifer and the Adjacent Layers*, *J. Hydr.*, 60, 311-328, 1983.
48. Tsang, Y. W., and P. A. Witherspoon, *Hydromechanical Behavior of a Deformable Rock Fracture Subject to Normal Stress*, *J. Geophys. Res.*, 86(B10), 9287-9298, 1981.
49. Whittle, P., *On Stationary Processes in the Plane*, *Biometrika*, 41, 434-449, 1954.
50. Witherspoon, P. A., C. H. Amick, J. E. Gale and K. Iwai, *Observations of a Potential Size Effect in Experimental Determination of the Hydraulic Properties of Fractures*, *Wat. Res. Res.*, 15(5), 1142-1146, 1979.
51. Witherspoon, P. A., J. S. Y. Wang, K. Iwai and J. E. Gale, *Validity of the Cubic Law for Fluid Flow in a Deformable Rock Fracture*, *Wat. Res. Res.*, 16(6), 1016-1024, 1980.